

© 2011 Rabie Abdullah Abu Saleem

EFFECTIVE THERMAL CONDUCTIVITY OF BINARY MIXED MATERIALS WITH  
FISSILE COMPONENTS—AN EMPIRICAL APPROACH

BY

RABIE ABDULLAH ABU SALEEM

THESIS

Submitted in partial fulfillment of the requirements  
for the degree of Master of Science in Nuclear, Plasma and Radiological Engineering  
in the Graduate College of the  
University of Illinois at Urbana-Champaign, 2011

Urbana, Illinois

Committee:

Professor Rizwan-uddin, Adviser  
Professor Magdi Ragheb

# ABSTRACT

An empirical approach to determine the effective thermal conductivity of a binary mixed material with heat generation is presented. Analysis was carried out for a steady state problem with spherical geometry to develop an expression for the effective thermal conductivity for the spherical pebble fuel in a pebble bed reactor. The approach is based on two main concepts: a structural approximation and an empirical formulation.

As for the structural approximation, the binary mixed material was assumed to be equivalent to a binary layered system of adjacent fuel and moderator layers oriented perpendicular to the direction of the heat flux. A model for heat transfer using an equivalent thermal conductivity in a binary mixture with no heat generation was developed. An assessment for this model was performed by comparing the effective thermal conductivity predicted by this model to some existing experimental data. Results from this evaluation showed good agreement between the experimental and the predicted values. It also showed that the less the difference between the thermal conductivities of the individual components, the better is the prediction for the effective thermal conductivity.

Next, an empirical formulation was developed for an expression for the effective thermal conductivity of a binary layered system *with* heat generation. This empirical formulation was analyzed systematically by considering the parametric and conditional effects of the system on the overall effective thermal conductivity. Some parameters were found to have no effect on the final expression of the thermal conductivity. These are the heat generation rate and the boundary conditions. Other parameters were found to significantly influence the value of the effective thermal conductivity. These are the abundance of individual components in the mixture and their thermal conductivities. This model yields a correlation for the thermal conductivity of the binary mixed material as:

$$k_h = \frac{k_f A_f + k_m A_m}{A_f + A_m}$$

With the modified volumetric ratios satisfy:

$$\frac{A_f}{A_m} = -196.105 \left( \frac{t_f}{t_m} \right)^2 + \left( 0.9 \frac{k_m}{k_f} + 13 \right) \frac{t_f}{t_m} - 0.1876 \quad \text{and} \quad (A_f + A_m) = 1$$

where  $k_f$  is the thermal conductivity for the first material with volumetric heat generation,  $k_m$  is the thermal conductivity for the second material with no volumetric heat generation, and  $\frac{t_f}{t_m}$  is the volumetric ratio of the first material to the second material.

Evaluation of this model was performed by comparing the predicted values of the effective thermal conductivity and temperature profiles with benchmark values. Results from this comparison showed that the empirical expression for the effective thermal conductivity developed here gives a better approximation for the heat conduction process in the layered system compared to the simple volume weighted thermal conductivity, which gives an unsatisfactory result.

The last step in the evaluation of the approach developed here was more comprehensive, in which the values predicted by the expression developed here for the effective thermal conductivity were compared to the values of effective thermal conductivity for the pebble fuel in a pebble bed reactor obtained using a correlation based on experimental data. This comparison showed satisfactory agreement between the two results with an average error of 18.41 percent.

## Acknowledgments

First and foremost, all my gratefulness is due to God Almighty for guiding me through to be able to complete this work. I would also like to thank my parents and family for all the support and encouragement, and for being my inspiration and the reason I seek knowledge.

Also, I would like to express my sincere gratitude for my advisor Professor Rizwan-uddin for his great support and patience throughout the entire work. I am thankful for his insight, guidance and encouragement. In addition, I highly appreciate the help and insight of Professor Magdi Ragheb and thank him for serving as a reader for this thesis.

I would also like to thank all my friends who shared with me the good times and the bad times through this journey. Finally, I would like to acknowledge all the faculty and staff of NPPE for their help and guidance.

# Table of Contents

## ACKNOWLEDGEMENTS

LIST OF TABLES .....	vii
----------------------	-----

LIST OF FIGURES .....	viii
-----------------------	------

CHAPTER 1. INTRODUCTION .....	1
-------------------------------	---

1.1 Heat Conduction and Thermal Conductivity .....	2
--	---

1.2 Pebble Bed Reactor and TRISO Fuel .....	3
---	---

CHAPTER 2. LITERATURE SURVEY .....	6
------------------------------------	---

2.1 Mixtures with no Heat Generation .....	6
--	---

2.1.1 Saturated Liquid-Solid System .....	6
---	---

2.1.2 Experimental Work for Mixtures of Porous Materials .....	8
--	---

2.2 Mixtures with Fissile Components .....	9
--	---

2.2.1 Two-Temperature Model for Pebble Fuel .....	9
---	---

2.2.2 The Correlation Reported by Gao and Shi [8].....	10
--	----

CHAPTER 3. EFFECTIVE THERMAL CONDUCTIVITY .....	12
---	----

3.1 Methodology .....	12
-----------------------	----

3.1.1 Modeling a Binary Mixed System (with no Heat Generation) as a Layered System	13
--	----

3.1.2 Simple Four Layers Problem with Heat Generation .....	16
---	----

3.1.2.1 Problem Description .....	16
-----------------------------------	----

3.1.2.2 Homogenization Methodology—Volume Weighted .....	17
--	----

3.1.2.3 Homogenization Methodology—Modified Volume Weighted .....	20
---	----

3.1.3 Modified Volumetric Ratios ( $A_f$ , $A_m$ ) for a Large Numbers of Layers .....	22
--	----

3.2 Parametric Study .....	25
----------------------------	----

3.2.1 Parameters with no effect on $k_h$ .....	25
--	----

3.2.2 Parameters that Affect $k_h$ .....	26
--	----

3.2.2.1 Dependency on Actual Volumetric Ratios of Fuel and Moderator .....	27
--	----

3.2.2.2	Dependency on Thermal Conductivities .....	30
3.3	Higher Order Fitting .....	32
CHAPTER 4.	RESULTS AND COMPARISON WITH PREVIOUS WORK.....	34
4.1	Heterogeneous Mixtures (Powdery Materials) with No Heat Generation .....	34
4.1.1	Mixture of fine sand and white lime .....	34
4.1.2	Mixture of fine sand and coal powder .....	36
4.1.3	Mixture of salt and sawdust .....	37
4.2	Fuel-Moderator Layered System .....	39
4.3	Fuel-Moderator Layered System Representing the PBMR Fuel .....	42
CHAPTER 5.	SUMMARY, CONCLUSIONS AND FUTURE WORK .....	46
5.1	Summary and Conclusions .....	46
5.2	Future Work .....	48
Appendix A.	Physical and Thermal Properties of Some Materials .....	49
Appendix B.	Experimental Thermal Conductivities for Mixtures of Porous Materials .....	53
Appendix C.	MatLab Code .....	55
Appendix D.	Analytical Solution for Temperature in Four-Layered Assembly (Figure 3.2) ...	59
References	.....	62

# LIST OF TABLES

Table 1.1: Material composition and typical dimensions of the TRISO particle .....	5
Table 3.1: Coefficients for the quadratic fit [Eq. (3.23)].....	33
Table 4.1: Thermal conductivity of mixture of fine sand and white lime at various volumetric fractions at 25 °C.....	35
Table 4.2: Thermal conductivity of mixture of fine sand and coal powder at various volumetric fractions at 25 °C.....	36
Table 4.3: Thermal conductivity of mixture of salt and sawdust at various volumetric fractions at 25 °C.....	38
Table 4.4: Average errors between the experimental value and the value predicted by the layered model for different binary mixed materials .....	39
Table 4.5: Volumetric ratios and thermal conductivities for 100-shells sphere (with the volumetric ratio of the fuel to the moderator ( $t_f/t_m$ ) equal to 0.0267).....	40
Table 4.6: Thermal conductivities of different types of graphite and thermal conductivity calculated using Eq. 2.9 at different temperatures .....	43
Table 4.7: Comparison of results for homogenized thermal conductivity with those predicted by the correlation reported by Gao and Shi [8].....	44

# LIST OF FIGURES

Figure 1.1: Fuel element design for a pebble bed reactor (a) Three dimensional (b) Two dimensional .....	4
Figure 2.1: Simple visualization for the series and parallel solid and liquid phase distributions considered by Woodside and Messmer [5] .....	6
Figure 2.2: Thermal conductivity for the pebble fuel (DOSIS = 0) as given by the correlation reported by Gao and Shi [8] .....	11
Figure 3.1: Schematic representation of a vertically layered slab .....	13
Figure 3.2: Schematic diagram for the four-layered system .....	16
Figure 3.3: Exact Temperature profile versus Temperature profile based on a volume-weighted thermal conductivity .....	19
Figure 3.4: Exact and homogenized temperature distributions for a four-layered slab .....	22
Figure 3.5: Convergence of the ratio ( $A_f/A_m$ ) as a function of number of layers .....	24
Figure 3.6: Relation between actual and modified volumetric ratios for a four-layered assembly ( $k_m/k_f = 21$ ) .....	28
Figure 3.7: Value of slope ( $m$ ) and the constant ( $C$ ) for different numbers of layers ( $N$ ) .....	29
Figure 3.8: Values of slope ( $m$ ) as a function of ( $k_m/k_f$ ) .....	31
Figure 3.9: Value of constant ( $C$ ) as a function of ( $k_m/k_f$ ) .....	31
Figure 4.1: Temperature profiles obtained using different estimates for the value of the thermal conductivity .....	41

# CHAPTER 1

## INTRODUCTION

In solids at low temperatures, heat is transferred mainly by conduction. The material property of *thermal conductivity* is used to quantify the conductive capabilities of different materials. For mixtures, the effective thermal conductivity depends on the composition of the constituent material, as well as the geometric arrangement. There are numerous engineering applications of materials composed of heterogeneous mixtures of two or more components. One of the most important examples of such materials in the nuclear power industry is the fuel used in the Pebble Bed Modular Reactor (PBMR). As is discussed in more detail below, there currently is no rigorous basis to determine an effective (or equivalent) thermal conductivity for a solid medium composed of finely dispersed particles of one kind of solid in a material with a very different thermal conductivity.

The goal of this research is to develop, using numerical experiments, a general expression for the thermal conductivity of a binary mixed material with a single fissile component, i.e., with heat being generated in one component of the mixture. Such an expression could be very useful, for example, to estimate the thermal conductivities of TRISO particles-based nuclear fuel. The rest of this chapter (Chapter 1) provides some introductory material on heat conduction and thermal conductivity. The structure of TRISO particles-based nuclear fuel, such as that used in the PBMR, is also described. A literature survey of earlier experimental and analytical work carried out in this field is presented in Chapter 2. The methodology to formulate the empirical expression for the thermal conductivity is developed in Chapter 3. The empirical expression developed in Chapter 3 is then evaluated in Chapter 4 using three different approaches, including comparison with experimental data from the literature. The summary and conclusions of this work are in Chapter 5, along with some suggestions for future work.

## 1.1 Heat Conduction and Thermal Conductivity

Conduction is one of the three fundamental modes of heat transfer. On a microscopic scale, heat conduction takes place when hot, vibrating atoms and molecules interact with their neighboring atoms and molecules, transferring some of their kinetic energy in the form of heat to the neighboring particles. Electrons also play a role in conduction for some solids. For solids at low temperatures, conduction is more significant than the other two modes of heat transfer, namely, convection and radiation.

The theory of thermal conductivity as proposed by Fourier in 1822 states that for a homogeneous solid, the local heat flux is proportional to the negative of the local temperature gradient. This can be mathematically represented by the Fourier law [1]:

$$\mathbf{q}'' = -k\nabla T \quad (1.1)$$

where  $\mathbf{q}''$  is the heat flux vector  $W/m^2$ ,  $k$  is the thermal conductivity of the material  $W/(m.K)$ , and  $\nabla T$  is the temperature gradient vector. (For anisotropic material,  $k$  is a tensor).

The negative sign in Eq. (1.1) indicates that the heat flux is considered positive in the direction of a negative temperature gradient. Thus, thermal energy is transported, or thermal energy *diffuses* along the gradient, from the regions of higher temperature to the regions of lower temperature.

The thermal conductivity of a material is therefore the heat transferred by conduction per unit area per unit time in the direction normal to the temperature gradient for a unit temperature gradient. For some materials, the thermal conductivity strongly depends upon temperature, thus presenting it as a nonlinear problem.

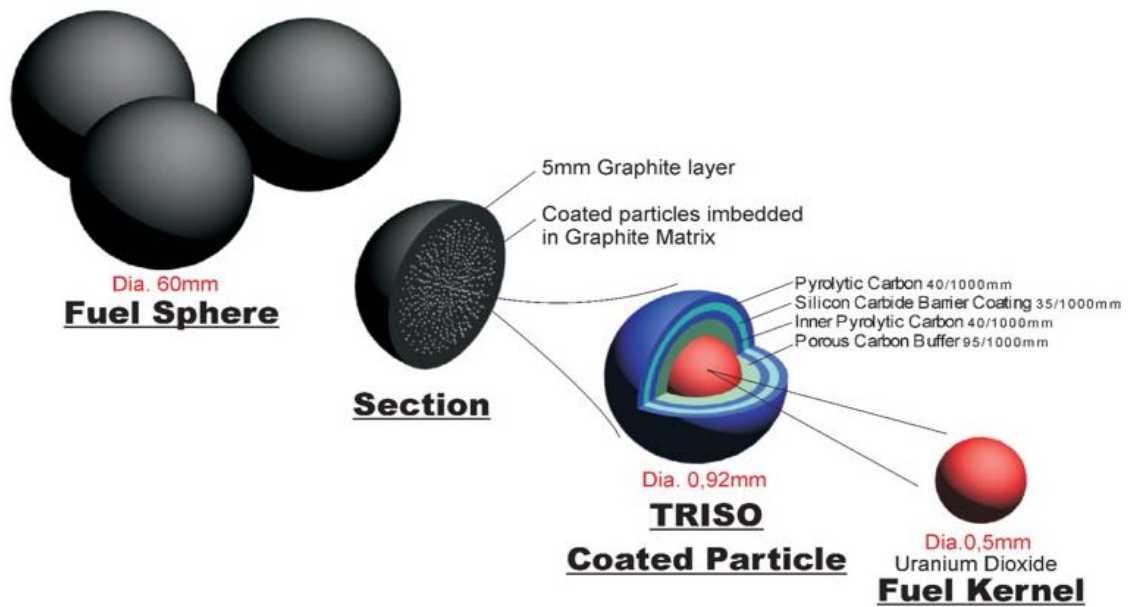
## 1.2 Pebble Bed Reactor and TRISO Fuel

In the PBMR, spherical fuel elements with a diameter of about 60 mm, about the size of a tennis ball, are used. Each sphere consists of an inner fuel region of 50 mm diameter containing the TRISO coated particles that are uniformly distributed in a dense graphite matrix. There can be up to 20,000 particles in a spherical fuel element. Each TRISO particle is coated with a special barrier coating, which ensures that radioactivity is kept locked inside the particle [4]. Surrounding the inner fueled zone is a 5 mm thick fuel-free shell made of the same high density graphite matrix, as shown in Fig. 1.1.

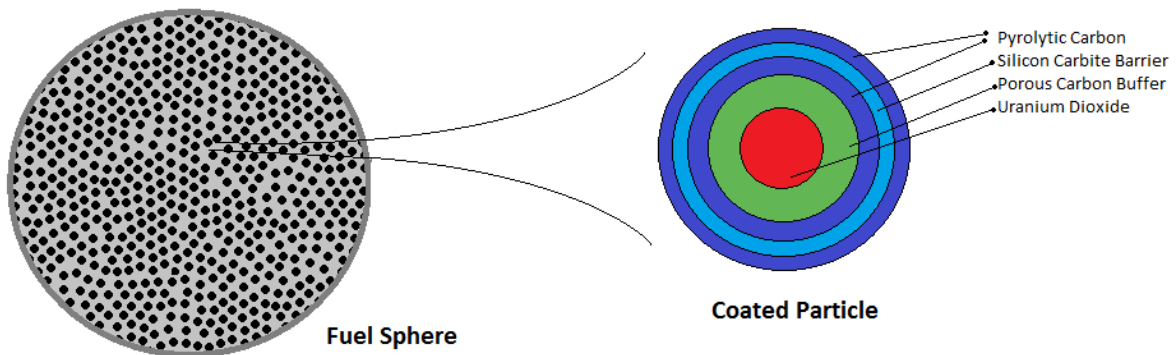
Coated fuel particles were originally proposed and designed in the DRAGON reactor project during the 1960s. These fuel particles provide the primary barrier to fuel and fission product migration [3].

As shown in Fig. (1.1), the TRISO particle is composed of a fuel kernel of uranium dioxide surrounded by a layer of porous carbon deposited on it [4]. This is followed by a thin coating of pyrolytic carbon (a very dense form of carbon), a layer of silicon carbide, and finally, another layer of pyrolytic carbon. Table (1.1) lists the material composition and typical dimensions of the TRISO particle.

The graphite matrix in the pebbles serves as the moderator as well as a structural material that provides another layer of protection and barrier. As for the composition of the graphite matrix, the standard A3-matrix (A3-3) performed well in the German AVR reactor starting in 1969. Another type of matrix graphite, which is a modification of the standard A3 graphite and is referred to as A3-27 graphite, has also performed well since 1976 [4]. Thermal properties of the two types of matrix graphite can be found in Appendix A.



(a)



(b)

Figure 1.1. Fuel element design for a pebble bed reactor.

(a) Three dimensional view [2] (b) Two dimensional cross sectional view.

Table 1.1. Material composition and typical dimensions of the TRISO particle [3, 11].

Region	Material	Thickness ( $\mu\text{m}$ )	Density (g/cc)	Thermal Conductivity W/(m.K)
Kernel	14% $UC_{0.5}O_{1.5}$	250	10.5	3.5
Buffer	Porous carbon	100	1.0	0.5
Inner PyC	Pyrolytic carbon	35	1.9	4.0
SiC	Silicon carbide	35	3.2	30
Outer PyC	Pyrolytic carbon	40	1.9	4.0

It is clear that the very small dimensions of the TRISO fuel particles would not allow numerical simulations on a grid so fine as to resolve each material separately. Hence, estimating the thermal properties of the heterogeneous mixture, or effective thermal properties of the pebble, is important.

## CHAPTER 2

### LITERATURE SURVEY

Several studies, both analytical and experimental, have been conducted to investigate the thermal conductivity of mixtures of different materials. Some of these examined the effective thermal conductivity of a mixture of different materials with no heat generated within the mixture, while other examined mixtures with fissile components. Some of these analytical and experimental studies are briefly reviewed in this chapter. Two studies, an analytical study and an experimental one, carried out for mixtures with no fissile components, are reviewed in the first section of this chapter. Two studies specifically carried out for the pebble bed fuel, which can be thought of as a mixture of two materials one of which is heat generating, are reviewed in the second section.

#### 2.1 Mixtures with no Heat Generation

##### 2.1.1 Saturated Liquid-Solid System

Thermal conductivity for a saturated liquid-solid system was studied by Woodside and Messmer in 1961 [5]. In their work, they considered two very simple phase distributions: the series and the parallel distributions. The two distributions gave two different expressions for the effective thermal conductivity of the system. Fig. (2.1) shows a simple schematic representation for the two distributions.

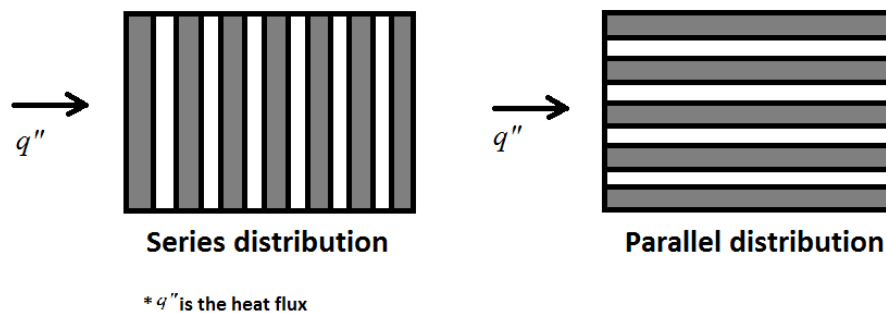


Figure 2.1. Simple visualization for the series and parallel solid and liquid phase distributions considered by Woodside and Messmer [5].

The parallel phase distribution, in which the two phases are thermally in parallel with respect to the direction of heat flow, leads to the maximum possible overall thermal conductivity (assuming that the solid's thermal conductivity is higher than the fluid's) given by:

$$k_{max} = \Phi k_{Fl} + (1 - \Phi)k_S \quad (2.1)$$

where:

$k_{Fl}$  = Thermal conductivity of fluid  $kcal/(m.h.^{\circ}C)$ .

$k_S$  = Thermal conductivity of solid  $kcal/(m.h.^{\circ}C)$ .

$\Phi$  = Porosity of the system.

This expression for thermal conductivity is based on simple volume weighted averaging of the two conductivities.

On the other hand, the series phase distribution, in which the two phases are thermally in series with respect to the direction of heat flow, leads to the minimum possible overall thermal conductivity given by:

$$k_{min} = \frac{k_{Fl}k_S}{\Phi k_S + (1 - \Phi)k_F} \quad (2.2)$$

As a result of their work, Woodside and Messmer found that the parallel system tends to over-estimate the experimental value of the effective thermal conductivity of the saturated liquid-solid system, while the series system tends to under-estimate [5]. Hence, they suggested an expression for thermal conductivity that leads to an intermediate value for the thermal conductivity as given by:

$$k_{int} = k_{Fl}^{\Phi} k_S^{1-\Phi} \quad (2.3)$$

This can also be expressed as:

$$\ln(k_{int}) = \Phi \ln(k_{Fl}) + (1 - \Phi)\ln(k_S) \quad (2.4)$$

Equation (2.4) predicts a linear relationship, on a ln-ln plot, between the effective conductivity of a liquid-filled porous medium and the conductivities of the solid and the liquid phases. This equation over-estimates the effective conductivity (experimental value) when  $k_S/k_{Fl}$  ratio exceeds 20 [5]. Note that this expression is suggested for domains with no heat generation.

### 2.1.2 Experimental work for Mixtures of Porous Materials

Thermal conductivity characteristics of binary mixtures of dry porous materials (powders or granular material) were investigated by Deng in 1992 [6]. An experiment was carried out to measure the thermal conductivities for mixtures of fine sand with white lime, fine sand with coal powder, and salt with sawdust at various volumetric mixing fractions, using a transient line-heat-source device. The transient line-heat-source system used was made from a Plexiglas container, an electric heating element, and two thermocouples.

Mixtures were oven-dried and screened with a 28 mesh Tyler sieve to obtain uniform-sized particles. Thermal-conductivity tests were completed at room temperatures. Results showed that, for the volumetric ratios studied, the low-conductivity material dominates the heat-conduction process in the binary mixture. It was found that the overall thermal conductivity dropped rapidly from the high to the low values when the volumetric fraction of the low conductivity material increased from 20% to 40% in the mixture. This means that mixing about 60% of the high-conductivity material with 40% of the low-conductivity material leads to an effective thermal-conductivity value that is closer to the thermal conductivity of the less thermally conductive material [6]. Results for this experiment are reported in Appendix B. Note that these results and conclusions are applicable to mixtures of “powdery” materials such as fine sand, white lime, coal powder, salt and sawdust.

## 2.2 Mixtures with Fissile Components

### 2.2.1 Two-Temperature Model for Pebble Fuel

This model was proposed by Cho et al. in 2009 [7] to solve the heterogeneous thermal problem of the fuel in a Very High Temperature Gas-cooled pebble-bed Reactor (VHTGR).

In this model, the graphite-plus-fuel region was thought of as a mixture of two distinct hypothetical materials occupying the same physical space. One material represents the fuel kernels characterized by the thermal conductivity  $k_f^i$  and temperature  $T_f^i$ . The other one represents the graphite matrix characterized by the thermal conductivity  $k_m^i$  and temperature  $T_m^i$  (the superscript  $i$  refers to the fact that the two media are imaginary or hypothetical).

Thermal responses of the two hypothetical materials (that occupy the same physical space) in this model are characterized by two coupled elliptic governing equations, with a coupling coefficient  $\mu$ . These equations are given by:

$$k_f^i \cdot \nabla^2 T_f^i(r, t) - \mu \cdot [T_f^i(r, t) - T_m^i(r, t)] + Q(t) = 0 \quad (2.5)$$

$$k_m^i \cdot \nabla^2 T_m^i(r, t) + \mu \cdot [T_f^i(r, t) - T_m^i(r, t)] = 0 \quad (2.6)$$

with:

$$Q(t) = \frac{\sum_i Q_i V_i}{V_{f-m}} \quad (2.7)$$

where:

$Q_i$  = volumetric heat generation rate of  $i$ -th fuel kernel  $\text{W}/\text{cm}^3$

$V_i$  = volume of  $i^{\text{th}}$  fuel kernel

$V_{f-m}$  = volume of fuel-graphite matrix

To complete the thermal model, the equation for the non-fueled graphite-only shell was also included:

$$k_g \cdot \nabla^2 T_g(r, t) = 0 \quad (2.8)$$

Equations (2.5), (2.6), and (2.8) were solved analytically applying the appropriate boundary conditions. Values for  $k_f^i$ ,  $k_m^i$  and  $\mu$  were determined by matching the analytical solutions with reference heterogeneous solutions provided by a Monte Carlo method.

### 2.2.2 The Correlation Reported by Gao and Shi [8]

Another study for the pebble fuel was carried in Germany. This study led to an empirical correlation to determine the effective thermal conductivity of a pebble fuel. The correlation represents the thermal conductivity as a function of both temperature and neutron radiation dose. The correlation as referred to by Gao and Shi [8] is given below:

$$k = 1.2768 \left[ 0.042 + 1.228 \times 10^{-4} T + \frac{0.06892 - 0.3906 \times 10^{-4} T}{0.105 + 1.931 \times 10^{-4} T + DOSIS} \right] \quad (2.9)$$

where  $k$  is the thermal conductivity W/(cm.K), DOSIS is fast neutron radiation dose ( $10^{21}n/cm^2$ ) and  $T$  is temperature ( $^{\circ}C$ ).

For un-irradiated fuel ( $DOSIS = 0$ ), thermal conductivity according to this correlation decreases with increasing temperature. Figure 2.2 shows the thermal conductivity plotted versus temperature with  $DOSIS = 0$ .

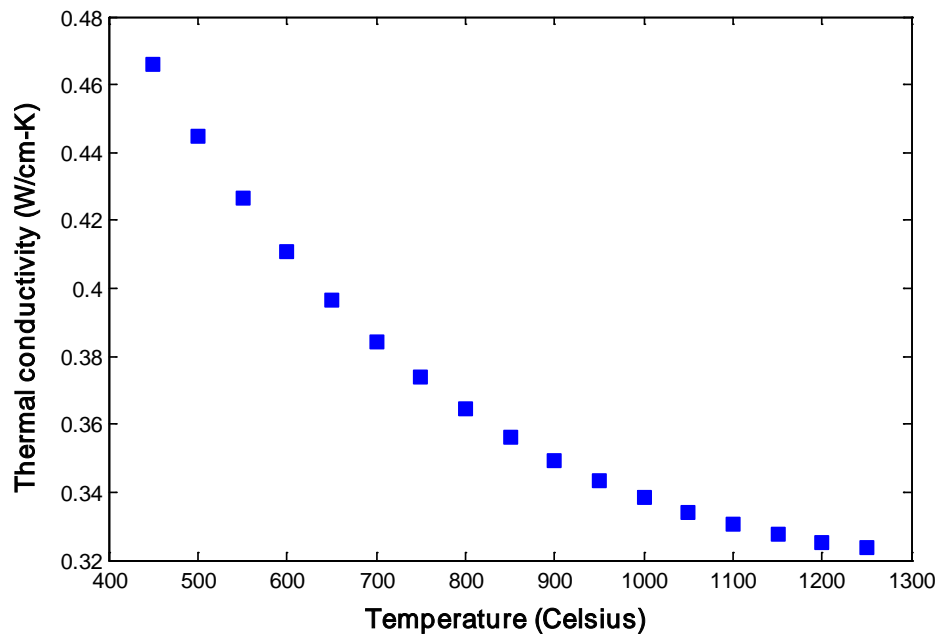


Figure 2.2. Thermal conductivity for the pebble fuel ( $DOSIS = 0$ ) as given by the correlation reported by Gao and Shi [8].

## CHAPTER 3

### EFFECTIVE THERMAL CONDUCTIVITY

In this chapter, an empirical approach is used to formulate an expression for the effective thermal conductivity of a binary mixed material with one fissile (heat generating) component. Taking advantage of the fact that the linear heat conduction equation can be solved even for highly heterogeneous media, an inverse problem is formulated to determine the effective thermal conductivity that would lead to minimizing the error between the temperature distributions found for the heterogeneous medium and that for the homogenized medium (with one effective thermal conductivity). The impact of several parameters is examined on the effective thermal conductivity. Results are then fitted into a final expression that can be used to find the effective thermal conductivity of a binary mixed material with one fissile component. The chapter first introduces the idea of approximating the heterogeneous system by a layered system. The idea of empirical formulation is then introduced by discussing a simple system of four layers. Finally, a parametric study is carried to find an expression for the effective (homogenized) thermal conductivity.

#### 3.1 Methodology

The methodology proposed here to develop an empirical expression for the effective thermal conductivity of a binary mixed system relies on the approximation that a heterogeneous medium of two uniformly mixed materials can be modeled as a number of one-dimensional, adjacent layers of the individual materials. Using this assumption, an empirical approach is employed to develop a general expression for the effective thermal conductivity of a layered medium. This expression is a function of different parameters such as the thermal conductivity of individual components, the abundance of each component, the heat generation rate and the boundary conditions.

### 3.1.1 Modeling a Binary Mixed System (with no Heat Generation) as a Layered System

As a structural approximation for the heterogeneous problem, a layered model is proposed. This model suggests that a heterogeneously mixed medium can be represented by an equivalent system of adjacent layers of the individual constituent materials. This will be similar to the phase distributions in series considered by Woodside and Messmer [5], discussed in Chapter 2.

In one dimensional Cartesian geometry, the system is a slab consisting of  $n$  vertical layers. Each layer can be of a different non-fissile material (no heat is generated in the system) and of different thickness  $dx_i$ . The system has a constant heat flux imposed on the left edge of the slab. Figure 3.1 shows this vertically layered system.

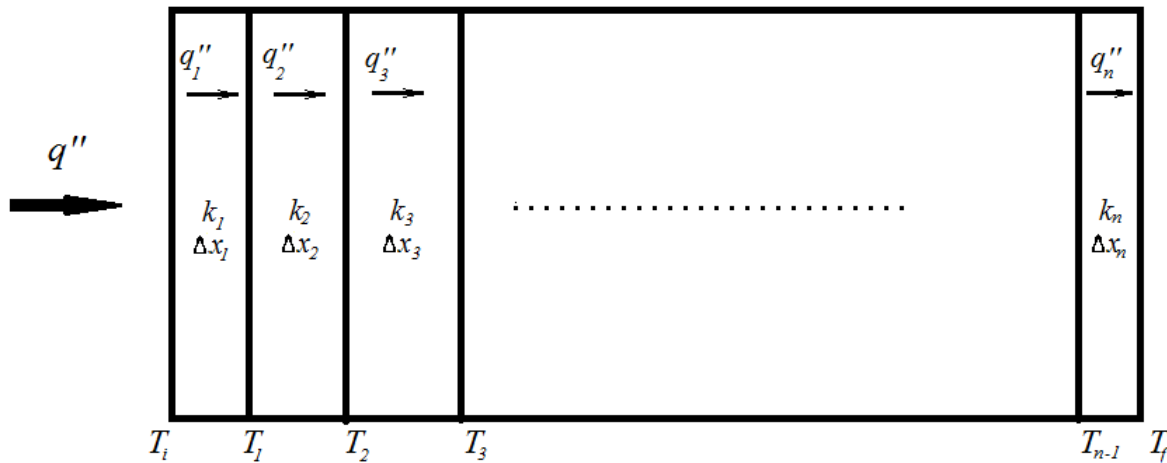


Figure 3.1. Schematic representation of a vertically layered slab.

Our goal is to determine an effective thermal conductivity  $k = k_{effV}$  for the entire (homogenized) slab, so that the energy conservation is respected and the temperature distribution

in the homogenized slab is *as close to the temperature distribution of the layered slab as possible*.

For no internal heat generation, and consequently, a linear temperature profile, Fourier's law can be used to solve for the heat flux:

$$q'' = -k_{\text{effV}} \frac{dT}{dx} \cong -k_{\text{effV}} \frac{\Delta T}{\Delta x} \quad (3.1)$$

where:

$$\Delta T = (T_f - T_i) = (\Delta T_1 + \Delta T_2 + \dots + \Delta T_n) \quad (3.2)$$

and  $\Delta x$  is the total thickness of the layered (and homogenized) slab.

Solving for  $\Delta T$  from Eq. (3.1) we get:

$$\Delta T \cong \frac{-q'' \Delta x}{k_{\text{effV}}} \quad (3.3)$$

The values  $\Delta T_1, \Delta T_2, \dots, \Delta T_n$  represent temperature differences across the individual layers.

We can also apply Fourier's law for each individual layer to get:

$$\Delta T_i \cong \frac{-q_i'' \Delta x_i}{k_i} \quad i = 1, 2, \dots, n. \quad (3.4)$$

Since thermal energy is conserved, we have

$$q_1'' = q_2'' = \dots = q_n'' = q'' \quad (3.5)$$

Substituting Eqs. (3.3), (3.4) and (3.5) into (3.2) and solving for  $k_{effV}$  we get:

$$k_{effV} \cong \frac{\Delta x}{\sum_{i=1}^n \frac{\Delta x_i}{k_i}} \quad (3.6)$$

The expression for the effective thermal conductivity given by Eq. (3.6) will lead to conservation of thermal energy; i.e. heat flux entering the model and leaving the model will be the same in the homogeneous problem as would occur in the heterogeneous problem (no heat generation case).

The general multi-material slab model shown in Fig. (3.1) can be reduced to represent a binary mixture of alternating layers made of only two constituent materials. For simplicity, thickness of each material is considered not to change from one layer to the next. Hence, these layers can be denoted by constant thicknesses,  $t_f$  and  $t_m$  and thermal conductivities,  $k_f$  and  $k_m$ , respectively. For such a system, Eq. (3.6) reduces to:

$$k_{effV} \cong \frac{t_f + t_m}{\left(\frac{t_m}{k_m}\right) + \left(\frac{t_f}{k_f}\right)}$$

$$k_{effV} \cong \frac{k_f k_m (t_f + t_m)}{t_m k_f + t_f k_m} \quad (3.7)$$

Equation (3.7) gives an approximation for the effective thermal conductivity of a binary mixed material with no heat generation. Note that while satisfying the conservation of energy requirement, this approach has left no room to optimize the temperature distribution in the homogenized system to match the temperature distribution of the heterogeneous system. A similar limitation exists even in multi-material problems when one material is generating heat.

### 3.1.2 Simple Four Layers Problem with Heat Generation

#### 3.1.2.1 Problem Description

To obtain a better understanding of the homogenization methodology, a simple slab of four alternating fuel-moderator layers was studied. This problem can be easily solved analytically to determine the temperature profile in the slab.

The assembly is composed of two fuel layers and two moderator layers, each of thickness  $a$ . The assembly is insulated on the left side (heat flux is zero on the left side), and the temperature on the right side is set to zero ( $T = 0$ ), with a constant volumetric power generation ( $Q$ ) in the fuel layers. The geometry and physical properties of this assembly are shown in Fig. (3.2).

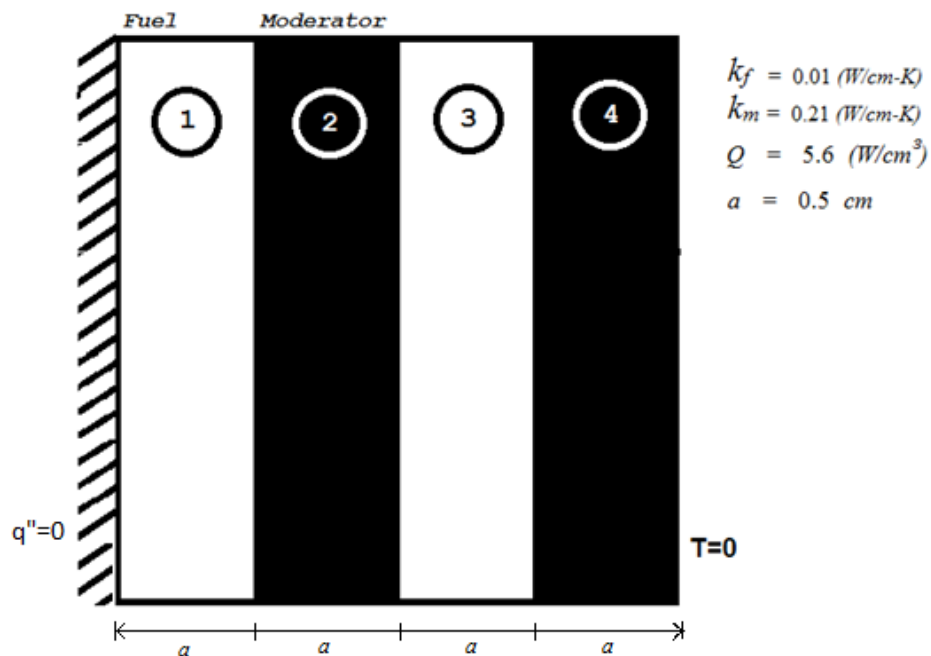


Figure 3.2. Schematic diagram for the four-layered system.

### 3.1.2.2 Homogenization Methodology—Volume Weighted

Temperature profiles in layers 1 through 4 are governed by the differential equation:

$$\frac{d^2 T_i}{dx^2} + \frac{Q_i}{k_i} = 0 \quad (3.8)$$

with the boundary conditions:

$$\left. \frac{dT_1}{dx} \right|_{x=0} = 0 \quad (3.9)$$

$$T_4|_{x=4a} = 0 \quad (3.10)$$

and the interface conditions:

$$k_j \left. \frac{dT_j}{dx} \right|_{x=j.a} = k_{j+1} \left. \frac{dT_{j+1}}{dx} \right|_{x=j.a} \quad (3.11)$$

$$T_j|_{x=j.a} = T_{j+1}|_{x=j.a} \quad (3.12)$$

where:

$$i = 1, 2, 3 \text{ and } 4$$

$$j = 1, 2 \text{ and } 3$$

$$Q_1 = Q_3 = Q = 5.6 \text{ W/cm}^3$$

$$Q_2 = Q_4 = 0$$

By solving the set of equations and boundary conditions above, we can obtain the exact temperature profile in the assembly, as shown below (Derivation details are shown in Appendix D):

$$T_1 = \left( \frac{-Q}{2k_f} \right) x^2 + a^2 Q \left( \frac{3}{k_m} + \frac{1}{2k_f} \right)$$

$$T_2 = \frac{-aQ}{k_m} x + \frac{4a^2 Q}{k_m}$$

$$T_3 = \left( \frac{-Q}{2k_f} \right) x^2 + \frac{aQ}{k_f} x + a^2 Q \left( \frac{3}{2k_f} + \frac{2}{k_m} \right)$$

$$T_4 = \frac{-2aQ}{k_m} x + \frac{8a^2 Q}{k_m}$$

The effective thermal conductivity for the whole assembly can be calculated in different ways. The simplest approach to determine the thermal conductivity for the homogenized system is to evaluate it as the volume weighted thermal conductivity of the constituent parts. For such an approach the expressions for both the thermal conductivity and the heat generation rate are given by:

$$k_{avg} = \frac{k_f t_f + k_m t_m}{t_f + t_m} \quad (3.13)$$

$$Q_{avg} = \frac{Q \cdot t_f}{t_f + t_m} \quad (3.14)$$

where  $t_f$  and  $t_m$  are the thicknesses of the fuel layer and the moderator layer, respectively.

The temperature distribution in the homogenized system is governed by:

$$\frac{d^2 T_{avg}(x)}{dx^2} + \frac{Q_{avg}}{k_{avg}} = 0 \quad (3.15)$$

with the same boundary conditions as used in the heterogeneous system Eqs. (3.9) and (3.10). Here,  $T_{avg}$  is the temperature profile in the homogenized system with a uniform (volume-weighted) thermal conductivity  $k_{avg}$  and uniform heat generation rate  $Q_{avg}$ . Once again, note that while satisfying the conservation of energy requirement, this approach has left no room to optimize the temperature distribution in the homogenized system to match the temperature distribution of the heterogeneous system.

Figure 3.3 shows the exact temperature profile in the assembly and the temperature profile for the homogenized system in which the (homogenized) thermal conductivity is determined by volume weighted averaging of the thermal conductivities of all the layers.

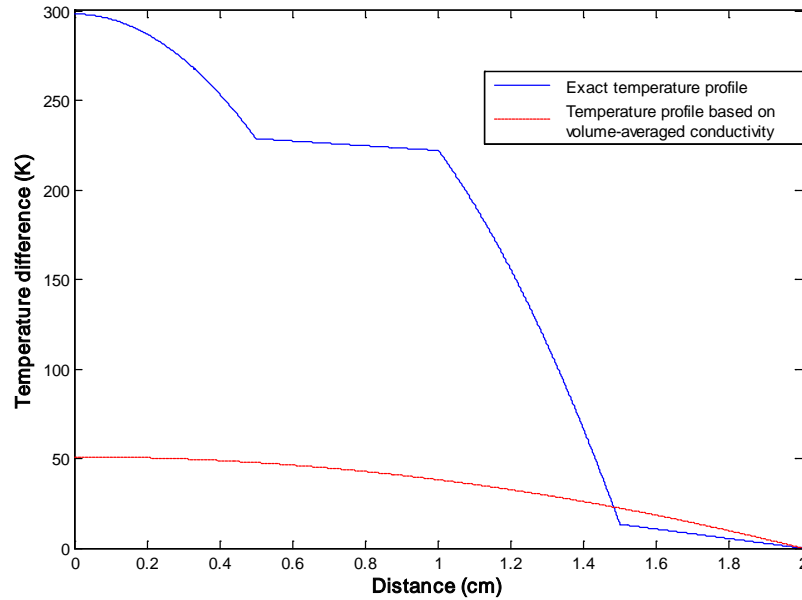


Figure (3.3). Exact Temperature profile versus Temperature profile based on a volume-weighted thermal conductivity.

Figure 3.3 clearly shows that the simple volume-averaging of thermal conductivities does not produce a good approximation for the temperature profile, and consequently does not represent a good homogenization approach for the heterogeneous medium.

### 3.1.2.3 Homogenization Methodology—Modified Volume Weighted

In this approach the same volume-averaging method is used as in Eq. (3.13), with the actual volumes of the two components  $t_f$  and  $t_m$  replaced by some as yet unspecified volumes  $A_f$  and  $A_m$ . The values for the modified volumes ( $A_f$  and  $A_m$ ) are to be chosen such that the temperature profile in the homogenized system matches the heterogeneous one; i.e. by minimizing the error between the approximate (homogenized) solution and the exact (heterogeneous) solution. The matching criterion also requires the areas under the two temperature profiles to be equal.

To keep the energy conserved,  $A_f$  and  $A_m$  are only employed in the equation for the thermal conductivity, but not in the evaluation of the average volumetric heat generation rate. To distinguish between the volume-weighted thermal conductivity and the modified thermal conductivity for the homogenized system (thermal conductivity evaluated using  $A_f$  and  $A_m$ ) the latter one is referred to as  $k_h$  given by:

$$k_h = \frac{k_f A_f + k_m A_m}{A_f + A_m} \quad (3.16)$$

where we normalize the modified volumetric ratio by requiring that:

$$(A_f + A_m) = 1 \quad (3.17)$$

By solving Eq. (3.15) using  $k_h$ , rather than  $k_{avg}$ , we get the quadratic temperature profile:

$$T_h = \left( \frac{-Q_{avg}}{2k_h} \right) x^2 + C_1 x + C_2 \quad (3.18)$$

Imposing the boundary condition 3.9 for  $T_h$ ,  $C_1$  is found to be zero.  $C_2$  can also be found by imposing the boundary condition 3.10, and its value is  $\left(\frac{8a^2 Q_{avg}}{k_h}\right)$ .  $Q_{avg}$  is given by Eq. (3.14).

To find  $k_h$ , the area under the approximate (homogeneous) temperature profile is required to be equal to the area under the exact (heterogeneous) temperature profile. The heterogeneous temperature profile was determined numerically using a MatLab code (found in Appendix C). The code was also used to match the areas under the two temperature profiles (the homogeneous in Eq. 3.18 and the heterogeneous found numerically) and calculate the value for  $k_h$  that makes the two areas equal. The optimum value for the effective thermal conductivity is found to be  $0.0235 \text{ W/(cm.K)}$ . Using Eqs. (3.16) and (3.17) with  $k_h$  is known we can solve for the modified volumes  $A_f$  and  $A_m$ .

Figure 3.4 shows both, the temperature profile in the homogenized system and the exact temperature profile in the assembly. Both of them are plotted for the entire thickness of the slab. It also shows the optimum values for  $A_f$  and  $A_m$ . The temperature distribution obtained using the homogenized thermal conductivity in this case, though in much better agreement with the exact temperature distribution compared to the simple volume weighted thermal conductivity case, still shows significant deviation.

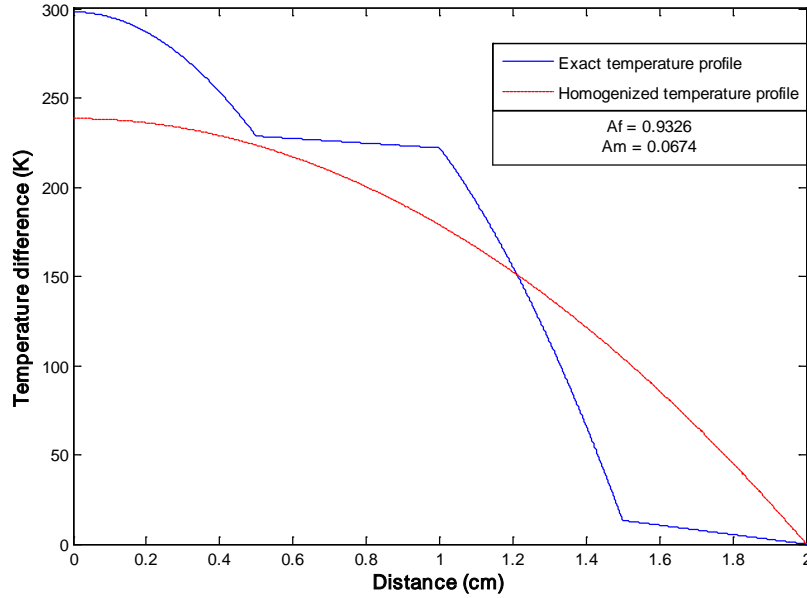


Figure 3.4. Exact and homogenized temperature distributions for a four-layered slab.

With the level of flexibility introduced in the modeling, this is the best that a single homogenized (effective) value for thermal conductivity can achieve. Clearly, this is not the most desirable formulation since the temperature variation in the homogenized system in several places is very far from the temperature in the heterogeneous system. However, the results reported above are for a four layer slab. In general, the heterogeneous systems that require homogenization have many more layers; i.e., in such systems the ratio of a characteristic unit cell to the characteristic system dimension is much smaller than unity. Results of homogenization for such a system are reported next.

### 3.1.3 Modified Volumetric Ratios ( $A_f$ , $A_m$ ) for a Large Numbers of Layers

A one-dimensional heterogeneous material is better represented by a layered (repeated-cell) system when the ratio of the repeating-cell's size to the size of the whole system is small. This requires the ratio  $(t_f + t_m)/L$  to be *small*, where  $t_f$  is the thickness of the fuel layer,  $t_m$  is the

thickness of the moderator layer, and  $L$  is the thickness of the whole system. The four layered slab studied above cannot be accurately represented by a homogeneous material. A heterogeneous system that can be better represented as a homogenized system would be a slab with a much smaller value for the ratio  $((t_f + t_m)/L)$ . (This ratio is 0.5 for the four layered system studied in Section 3.1.2.3.)

Two possible approaches to reduce this ratio are: 1) by decreasing the thicknesses of individual layers, or 2) increasing the size of the system. To simplify the analysis and associated computer coding  $(t_f + t_m)$  is required to satisfy:

$$(t_f + t_m) = 1.$$

Hence, the ratio  $((t_f + t_m)/L)$  is made smaller by increasing  $L$ , i.e., by increasing the number of layers in the system.

With length of the domain (or number of repeating layers) as a modeling parameter, it is important to analyze the impact of this parameter on the accuracy of the homogenization approximation. It would be expected that as the number of repeating layers in the system is increased, the modified volumetric ratio that would lead to the best temperature fit would approach a constant value. For this purpose, the analysis in section 3.1.2.3 is carried out for an increasing number of layers. The results are shown in Fig. (3.5). It shows the optimum value for the ratio  $A_f/A_m$  calculated for different numbers of layers. As expected, the best modified volumetric ratio approaches a constant value.

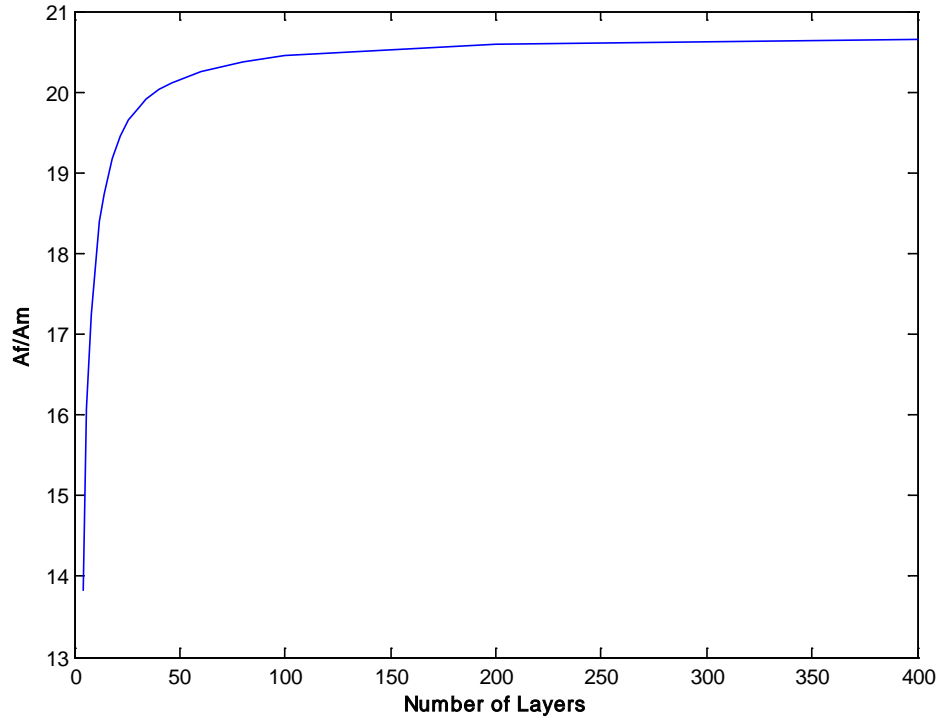


Figure 3.5. Convergence of the ratio ( $A_f/A_m$ ) as a function of number of layers.

It is clear that the optimum value for  $A_f/A_m$  approaches a near constant value for nearly 100 layers or more. This value is approximately 20.75. Hence, based on this numerical experiment, it can be concluded that heterogeneous systems with a number of repeating layers close to 100 or more can be well represented by a homogenized (or effective) thermal conductivity.

### 3.2 Parametric Study

The homogenized thermal conductivity as proposed in Eq. (3.16) can be a function of different parameters; such as:

- 1- Heat generation rate.
- 2- Boundary conditions.
- 3- Abundance of individual components.
- 4- Thermal conductivity of each component.

This dependency is expected to be reflected in the optimal values for the modified volumetric ratios  $A_f$  and  $A_m$ .

The influence of the four parameters mentioned above on the optimal values for  $A_f$  and  $A_m$  is investigated. The study is carried out for a spherical geometry rather than cartesian (so the results will be more relevant to a pebble bed fuel). The system is approximated by a repeating cell composed of two alternating shells of fuel and moderator in a one-dimensional spherical coordinate system, with heat transfer taking place in the radial direction only.

#### 3.2.1 Parameters with no effect on $k_h$

A study is carried out to examine the effect of heat generation rate and the type of boundary condition on the optimum value for  $(A_f/A_m)$ . For an assembly of 100 shells the ratio  $(t_f/t_m)$  was kept fixed at 0.015, with a fuel thermal conductivity of 0.01 W/(cm.K) and a moderator thermal conductivity of 0.21 W/(cm.K).

Optimum values for the ratio  $(A_f/A_m)$  were determined for a range of values of the volumetric heat rate  $(Q)$ . Simulations were carried out for  $0.5 < Q < 50 \text{ W/cm}^3$ . This numerical experiment

showed that the ratio ( $A_f/A_m$ ) remains nearly unchanged ( $\sim 0.24$ ) over the entire range of  $Q$  values used in these simulations.

Boundary conditions were also considered in this parametric analysis. Adiabatic boundary condition was imposed at the center. Two types of boundary conditions were considered for the outer surface of the system:

- 1- Dirichlet boundary condition (where the temperature is specified.)
- 2- Robin mixed boundary condition (where a linear combination of the temperature and the heat flux is specified.)

Both types of boundary conditions resulted in the same optimum value for the ratio ( $A_f/A_m$ ).

### 3.2.2 Parameters that Affect $k_h$

The homogenized or effective thermal conductivity of a heterogeneous material is expected to depend on:

- 1- The abundance of individual components
- 2- The thermal conductivity of each component.

This dependency is reflected on the optimum value for the modified volumetric ratios,  $A_f$  and  $A_m$ .

### 3.2.2.1 Dependency on Actual Volumetric Ratios of Fuel and Moderator

The actual fuel-thickness to moderator-thickness ratio ( $t_f/t_m$ ) represents the relative physical abundance of the fuel and the moderator in the mixed material.

In order to examine how the optimum value for the modified volumetric ratio ( $A_f/A_m$ ) depends on the actual abundance of the individual components, simulations were carried out for different values for the ratio ( $t_f/t_m$ ). Analysis was carried out for a spherical geometry of four shells 0.5 cm each, keeping the thermal conductivities of fuel and moderator to be  $k_f = 0.01$  W/(cm.K) and  $k_m = 0.21$  W/(cm.K) respectively, and the heat generation rate in the fuel layers  $Q = 5.6$  W/cm<sup>3</sup>. The boundary conditions used in this parametric analysis are given by Eqs (3.9) and (3.10).

Figure 3.6 shows the modified volumetric ratio for a four-layered assembly as a function of the actual ratio ( $t_f/t_m$ ) for  $k_m/k_f = 21$ . It also shows a linear fit through the data. This fit was determined using MatLab based on the method of least squares. The linear relation between the two variables is given by:

$$\frac{A_f}{A_m} = 0.88 + 40 \frac{t_f}{t_m}$$

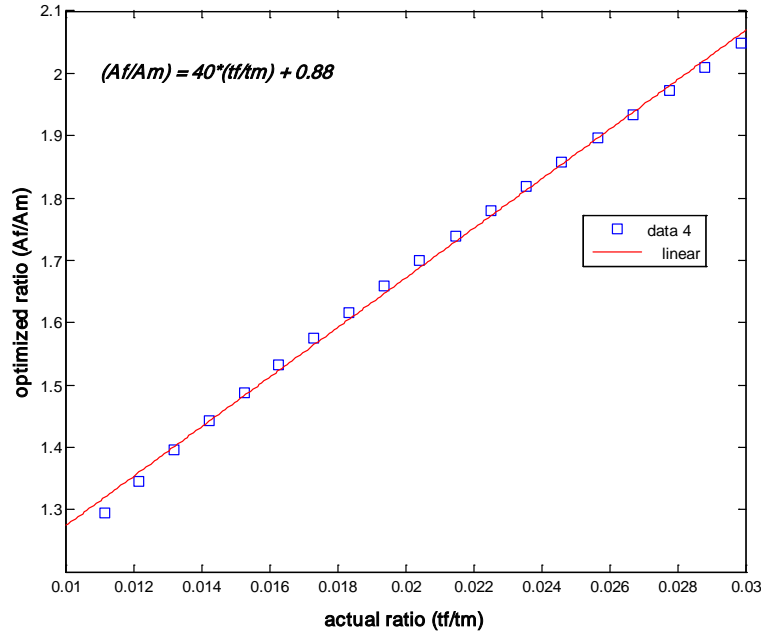


Figure 3.6. Relation between actual and modified volumetric ratios for a four-layered assembly

$$(k_m/k_f = 21).$$

As discussed in section 3.1.3, representing the heterogeneous system by a larger number of layers gives a better representation for the homogenized material. Hence, the relation between the actual and modified volumetric ratios was represented in general as:

$$\frac{A_f}{A_m} = C + m \frac{t_f}{t_m} \quad (3.19)$$

where  $m$  is the slope,  $C$  is a constant.

The slope ( $m$ ) and the constant ( $C$ ) will vary with the number of repeating layers used in the homogenization study. Moreover, as in Section (3.1.3), it is expected that the values for  $m$  and  $C$  will approach their limiting values as the number of layers in the analysis reported above (for four layer system) is increased. Values of  $m$  and  $C$  are plotted as a function of number of

repeating layers in Fig. (3.7). (Note that the number of repeating cells in any simulation is nearly half the number of layers.)

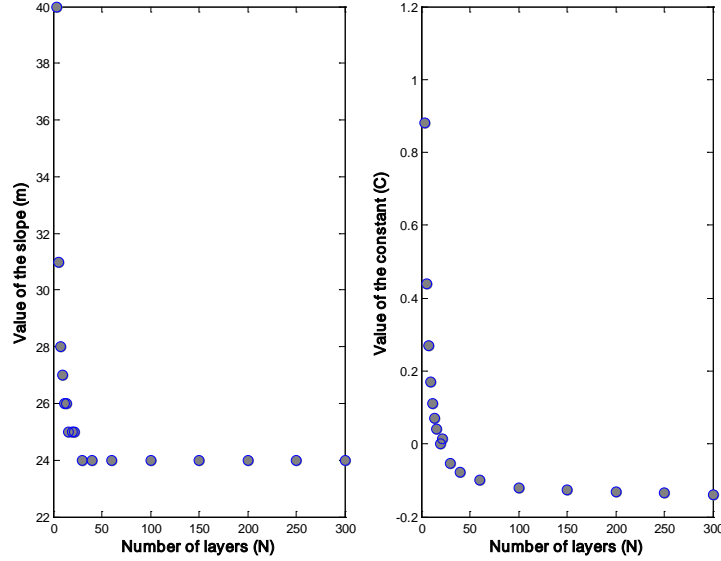


Figure 3.7. Value of slope ( $m$ ) and the constant ( $C$ ) for different numbers of layers ( $N$ ).

Results in Fig. (3.7) show the same convergence behavior as that found in section 3.1.3. A slope  $m = 24$  and constant  $C = -0.14$  capture the relationship between the actual and modified volumetric ratios data for a large number of repeating layers ( $N > 100$ , with 50 or more repeating cells). (Some data points in Fig. (3.7) do not show a smooth behavior. This is due to the fact that the data for this figure are based on a linear fit for the actual and modified volumetric ratios data.)

Substituting these values for  $m$  and  $C$  into Eq. (3.19), gives the final linear relation between the actual volumetric ratios and the optimum value for the modified volumetric ratios:

$$\frac{A_f}{A_m} = 24 \frac{t_f}{t_m} - 0.14 \quad (3.20)$$

This relationship is optimized for different volumetric ratios of the two materials as well as for the number of repeating cells.

### 3.2.2.2 Dependency on Thermal Conductivities

Values for the slope  $m$  and the constant  $C$  in Eq. (3.19) can still be dependent on other parameters. The last parameter considered in this study is the effect of thermal conductivities of the composing materials.

The MatLab code written for this purpose was run for a range of values of the fuel thermal conductivity  $k_f$  and the moderator thermal conductivity  $k_m$ . Values for the slope  $m$  and the constant  $C$  were then examined.

Values for the slope  $m$  are plotted against the ratio between the thermal conductivities of the moderator and the fuel, namely  $k_m/k_f$ . Figure 3.8 shows both the data and a linear fit for this data. The linear fit is given by:

$$m = 0.95 \frac{k_m}{k_f} + 4.9 \quad (3.21)$$

Values for the constant ( $C$ ) are also examined. Figure 3.9 shows the constant  $C$  plotted against the ratio ( $k_m/k_f$ ). It also shows the average value (-0.10797) about which the value of  $C$  was oscillating. Both fits were determined using MatLab, based on the method of least squares.

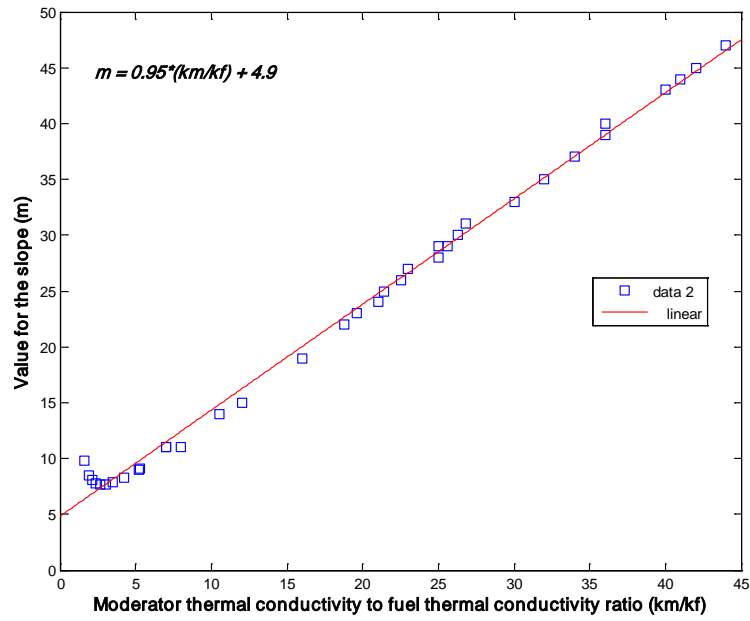


Figure 3.8. Values of slope ( $m$ ) as a function of  $(k_m/k_f)$ .

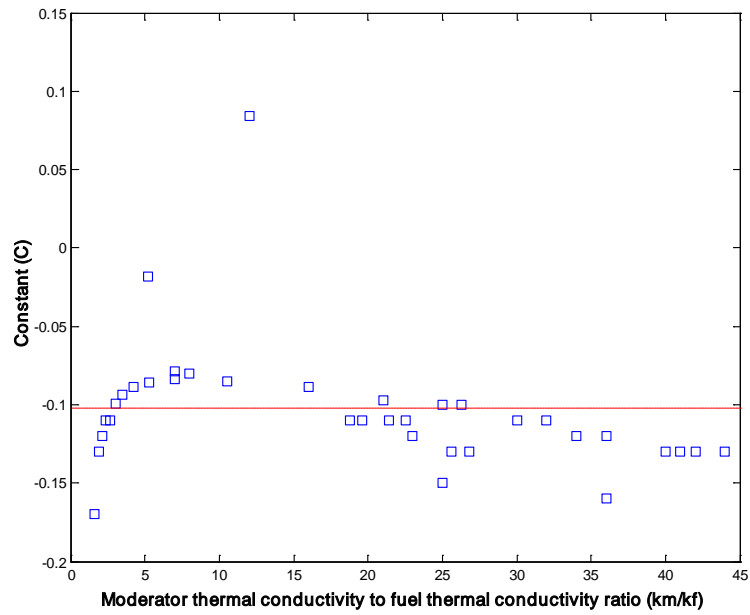


Figure 3.9. Value of constant ( $C$ ) as a function of  $(k_m/k_f)$ .

This leads to the final expression for the optimum value of the modified fuel to moderator volumetric ratio ( $A_f/A_m$ ) that does account for the effects of the actual volumetric ratios as well as the effect of thermal conductivities of the two constituting components:

$$\frac{A_f}{A_m} = \left[ \left( 0.95 \frac{k_m}{k_f} + 4.9 \right) \frac{t_f}{t_m} \right] - 0.10797 \quad (3.22)$$

For given thermal conductivities and volumetric ratios of the two materials, this expression can be used to solve for the homogenized thermal conductivity  $k_h$  given by Eq. (3.16).

### 3.3 Higher Order Fitting

The data shown in Fig. (3.6) are fitted with a linear fit using Eq. (3.19). However, as can be seen, the data in Fig. (3.6) have a slight curvature and can be better fitted with a quadratic profile. For the quadratic fit, the optimum value of the modified volumetric ratio can be expressed as:

$$\frac{A_f}{A_m} = C_3 \left( \frac{t_f}{t_m} \right)^2 + C_4 \left( \frac{t_f}{t_m} \right) + C_5 \quad (3.23)$$

The constants,  $C_3$ ,  $C_4$  and  $C_5$ , are however expected to change as the thermal conductivities of the individual components, represented by the ratio  $k_m/k_f$ , are changed.

Values for the constants  $C_3$ ,  $C_4$  and  $C_5$  given by the quadratic fit to the data in Fig. (3.6) are evaluated for different values of the ratio  $k_m/k_f$  (just like the slope ( $m$ ) and the constant ( $C$ ) in section 3.2.2.2). That is, data presented in Fig. (3.6) for  $k_m/k_f = 21$ , are generated for 36 different values of  $k_m/k_f$  ( $1.6 < k_m/k_f < 44$ ). For each value of  $k_m/k_f$ , values for the constants  $C_3$ ,  $C_4$  and  $C_5$  are evaluated by curve fitting the data with a quadratic function. It was

noticed that only  $C_4$  varied with  $k_m/k_f$ , while  $C_3$  and  $C_5$  remained nearly unchanged. Values of  $C_3$  and  $C_5$  and the near-linear variation of  $C_4$  with  $k_m/k_f$  are reported in Table (3.1).

Table 3.1. Coefficients for the quadratic fit [Eq. (3.23)].

$C_3 = -196.105$
$C_4 = 0.9 \left( \frac{k_m}{k_f} \right) + 13$
$C_5 = -0.1876$

Hence, the expression for the optimum value of the modified fuel to moderator volumetric ratio ( $A_f/A_m$ ) based on a parabolic fit is:

$$\frac{A_f}{A_m} = -196.105 \left( \frac{t_f}{t_m} \right)^2 + \left( 0.9 \frac{k_m}{k_f} + 13 \right) \frac{t_f}{t_m} - 0.1876 \quad (3.24)$$

Equations (3.22) and (3.24) do not explicitly depend on temperature; nevertheless this dependency is implicit via the thermal conductivities of the composing materials.

Equations (3.22) and (3.24) can be used to determine the optimum value of the modified volumetric ratio ( $A_f/A_m$ ). This, in turn, can be substituted in Eq. (3.16) to calculate the effective thermal conductivity of a binary mixed material with one fissile component. These empirical correlations are used and the resulting thermal conductivities are compared against some existing data in the next chapter.

## CHAPTER 4

### RESULTS AND COMPARISON WITH PREVIOUS WORK

The correlations developed in Chapter 3 are analyzed by comparing their results against some existing experimental data. Three levels of analyses are carried out here. The first one is to test the layered model against experimental data for heterogeneous mixtures of powdery materials with no heat generation. The second level is for a binary layered system with one fissile component. Results for this case are compared against “exact” analytical solutions. The final level of analysis is a more comprehensive test applied to a binary uniformly mixed system with one fissile component. Results for the layered model are compared against values of thermal conductivity for a pebble bed fuel obtained using an experimentally determined correlation.

#### 4.1 Heterogeneous Mixtures (Powdery Materials) with No Heat Generation

As a structural approximation for any binary mixed material, the layered system model discussed in section 3.1.1 is validated in this section against some existing data for the no heat generation case. Equation (3.7) is used to evaluate the effective thermal conductivity for the three binary mixed materials studied by Deng [6]. The results are compared against the experimental values for the effective thermal conductivities as measured by Deng [6]. Note that these cases are for two powder-like materials mixed in different proportions.

##### 4.1.1 Mixture of fine sand and white lime

A mixture of fine sand with thermal conductivity of  $0.391 \text{ W/(m.K)}$  [ $0.336 \text{ kcal/(hr.m.}^{\circ}\text{C)}$ ], and white lime with thermal conductivity of  $0.226 \text{ W/(m.K)}$  [ $0.194 \text{ kcal/(hr.m.}^{\circ}\text{C)}$ ], at a temperature of  $25^{\circ}\text{C}$  was considered first. Table (4.1) shows the volumetric fraction of fine sand in the mixture in the first column. The second column shows the effective thermal conductivity as predicted by the model developed in Chapter 3 (Eq. 3.7). Experimental results for the effective

thermal conductivity of the mixture as found by Deng [6] are shown in the third column. The last column of the table shows the relative error between the two values of thermal conductivity for the different volumetric fractions. Values for the error range between a minimum of 0.62 percent and a maximum of 17.62 percent, and the average error is found to be 7.49 percent.

Table 4.1. Thermal conductivity of mixture of fine sand and white lime at various volumetric fractions at 25 °C [6].

Volumetric fraction of fine sand	Effective thermal conductivity $kcal/(hr.m.^{\circ}C)^{*}$ (model)	Effective thermal conductivity $kcal/(hr.m.^{\circ}C)^{*}$ (experimental)	Relative error (percent)
0.000	0.194	0.194	0.00
0.091	0.202	0.194	4.00
0.167	0.209	0.200	4.37
0.375	0.231	0.196	17.62
0.444	0.239	0.220	8.55
0.500	0.246	0.221	11.30
0.526	0.249	0.224	11.36
0.556	0.254	0.222	14.23
0.588	0.258	0.250	3.26
0.625	0.264	0.262	0.62
0.667	0.270	0.292	7.48
0.714	0.278	0.301	7.70
0.769	0.287	0.313	8.18
0.833	0.299	0.311	3.73
0.909	0.315	0.323	2.47
1.000	0.336	0.336	0

\*1  $kcal/(hr.m.^{\circ}C) = 1.163 W/(m.K)$

#### 4.1.2 Mixture of fine sand and coal powder

A mixture of fine sand and coal powder with thermal conductivity of  $0.231 \text{ W/(m.K)}$  [ $0.199 \text{ kcal/(hr.m.}^\circ\text{C)}$ ] at a temperature of  $25^\circ\text{C}$  was also considered. Results are tabulated in Table (4.2).

Table 4.2. Thermal conductivity of mixture of fine sand and coal powder at various volumetric fractions at  $25^\circ\text{C}$ .

Volumetric fraction of fine sand	Effective thermal conductivity $\text{kcal/(hr.m.}^\circ\text{C)}$ * (model)	Effective thermal conductivity $\text{kcal/(hr.m.}^\circ\text{C)}$ * (experimental)	Relative error (percent)
0.000	0.199	0.199	0.000
0.091	0.207	0.208	0.640
0.231	0.220	0.208	5.621
0.375	0.235	0.223	5.345
0.500	0.250	0.230	8.678
0.526	0.253	0.237	6.891
0.556	0.257	0.243	5.901
0.588	0.262	0.253	3.461
0.625	0.267	0.271	1.456
0.667	0.273	0.277	1.322
0.714	0.281	0.285	1.499
0.769	0.290	0.311	6.785
0.833	0.301	0.321	6.120
0.909	0.316	0.332	4.762
1.000	0.336	0.336	0.000

\*1  $\text{kcal/(hr.m.}^\circ\text{C)} = 1.163 \text{ W/(m.K)}$

Values for the volumetric fraction of fine sand are shown in the first column. The effective thermal conductivity as predicted by the layered model and the experimental value determined by Deng [6] are given in the second and the third columns, respectively. The relative error between the two values is in the last column.

Values of the error for this mixture ranged between a minimum of 0.64 percent and a maximum of 8.678 percent, and the average error was found to be 4.5%.

#### 4.1.3 Mixture of salt and sawdust

The thermal conductivity of a mixture of salt with thermal conductivity of  $0.458 \text{ W/(m.K)}$  [ $0.394 \text{ kcal/(hr.m.}^{\circ}\text{C)}$ ], and sawdust with thermal conductivity of  $0.0954 \text{ W/(m.K)}$  [ $0.082 \text{ kcal/(hr.m.}^{\circ}\text{C)}$ ] was also modeled. The results are tabulated in Table (4.3). In this table, the first column shows the volumetric fraction of salt in the mixture. The effective thermal conductivity as predicted by the layered model and found experimentally by Deng [6] is shown in the second and the third columns, respectively. The relative error between the two values is shown in the last column.

The error for this mixture was the highest and ranged between a minimum of 4.539 percent and a maximum of 36.828 percent, and the average error was found to be 22.666 percent.

Table 4.3. Thermal conductivity of mixture of salt and sawdust at various volumetric fractions at 25 °C.

Volumetric fraction of salt	Effective thermal conductivity $kcal/(hr.m.^{\circ}C)^*$ (model)	Effective thermal conductivity $kcal/(hr.m.^{\circ}C)^*$ (experimental)	Relative error (percent)
0.000	0.082	0.082	0.000
0.091	0.088	0.099	10.740
0.231	0.100	0.096	4.539
0.333	0.111	0.131	14.987
0.412	0.122	0.159	23.454
0.500	0.136	0.177	23.306
0.526	0.141	0.165	14.825
0.555	0.146	0.191	23.405
0.588	0.153	0.217	29.286
0.625	0.162	0.257	36.828
0.666	0.174	0.243	28.599
0.714	0.189	0.263	28.259
0.769	0.210	0.288	27.190
0.833	0.241	0.338	28.723
0.909	0.293	0.381	23.185
1.000	0.394	0.394	0.000

\*1  $kcal/(h.m.^{\circ}C) = 1.163 W/(m.K)$

Table (4.4) summarizes some of the key findings for the three different mixtures reported above. In addition to the average relative error in thermal conductivity, the table in the last column shows the ratio of the thermal conductivities of the individual components of each mixture ( $k_1/k_2$ ). Results in Table (4.4) suggests that the model developed in Chapter 3 works better for mixtures when the thermal conductivities of the two composing materials are close in magnitude to each other ( $0.5 < (k_1/k_2) < 2$ ). This can be understood on the basis that heat flow follows the path of least resistance in the material with a much higher conductivity than the other material in the binary mixed medium.

Table 4.4. Average errors between the experimental value and the value predicted by the layered model for different binary mixed materials.

Binary mixed material	Averaged relative error percent	Ratio of thermal conductivities of the individual components, ( $k_1 / k_2$ )
Salt and sawdust	22.67	4.8
Fine sand and white lime	7.5	1.73
Fine sand and coal powder	4.5	1.693

## 4.2 Fuel-Moderator Layered System

Expressions given by Eqs. (3.22) and (3.24) are used to evaluate the optimal value for the modified volumetric ratio ( $A_f/A_m$ ). This, in turn, is used to evaluate the homogenized thermal conductivity given by Eq. (3.16) for any binary layered system of fuel and moderator. These expressions are used to determine the homogenized conductivity for a specific case of a binary layered sphere, and to compare the resulting temperature distribution with the exact temperature distribution.

The homogenization procedure developed in Chapter 3 is applied to determine the homogenized thermal conductivity and the temperature profile in a binary layered (shelled) spherical system of 100 layers. The sphere is composed of 0.026 cm fuel layers of 0.01 W/(m.K) thermal conductivity and 0.974 cm moderator layers of 0.21 W/(m.K) thermal conductivity. Note that the thermal conductivity ratio of the two materials is 21.

Using Eq. (3.16), the homogenized thermal conductivities  $k_{h1}$ ,  $k_{h2}$  were calculated using the volumetric ratios as given by Eqs. (3.22) and (3.24) respectively. The effective thermal conductivity  $k_{effv}$  given by Eq. (3.7) was also calculated along with the volume weighted thermal conductivity  $k_{avg}$  given by Eq. (3.13). All those thermal conductivities are shown in

Table (4.5). Also tabulated is  $k_{match}$  which is the thermal conductivity that would give a quadratic temperature profile under which the area is equal to the area under the exact temperature profile for the binary layered sphere.  $k_{match}$  is considered to be the reference value and errors are calculated relative to  $k_{match}$ . Errors are tabulated in the last column. Note that despite the large difference in the thermal conductivities of the two materials, the estimated thermal conductivities of the homogenized material, except for the simple volume-weighted case, are fairly accurate.

Table 4.5. Volumetric ratios and thermal conductivities for 100-shells sphere (with the volumetric ratio of the fuel to the moderator ( $t_f/t_m$ ) equal to 0.0267).

Thermal conductivity	Value W/(m.K)	Error from $k_{match}$ (percent)
$k_{match}$ (by matching with heterogeneous solution)	0.1439	0.0
$k_{avg}$ (given by Eq. 3.13)	0.2049	42.4
$k_{effV}$ (given by Eq. 3.7)	0.1391	3.34
$k_{h1}$ (given by Eq. 3.22)	0.1397	2.9
$k_{h2}$ (given by Eq. 3.24)	0.1422	1.18

The temperature profiles obtained using different values of the thermal conductivity are plotted in Fig. (4.1).

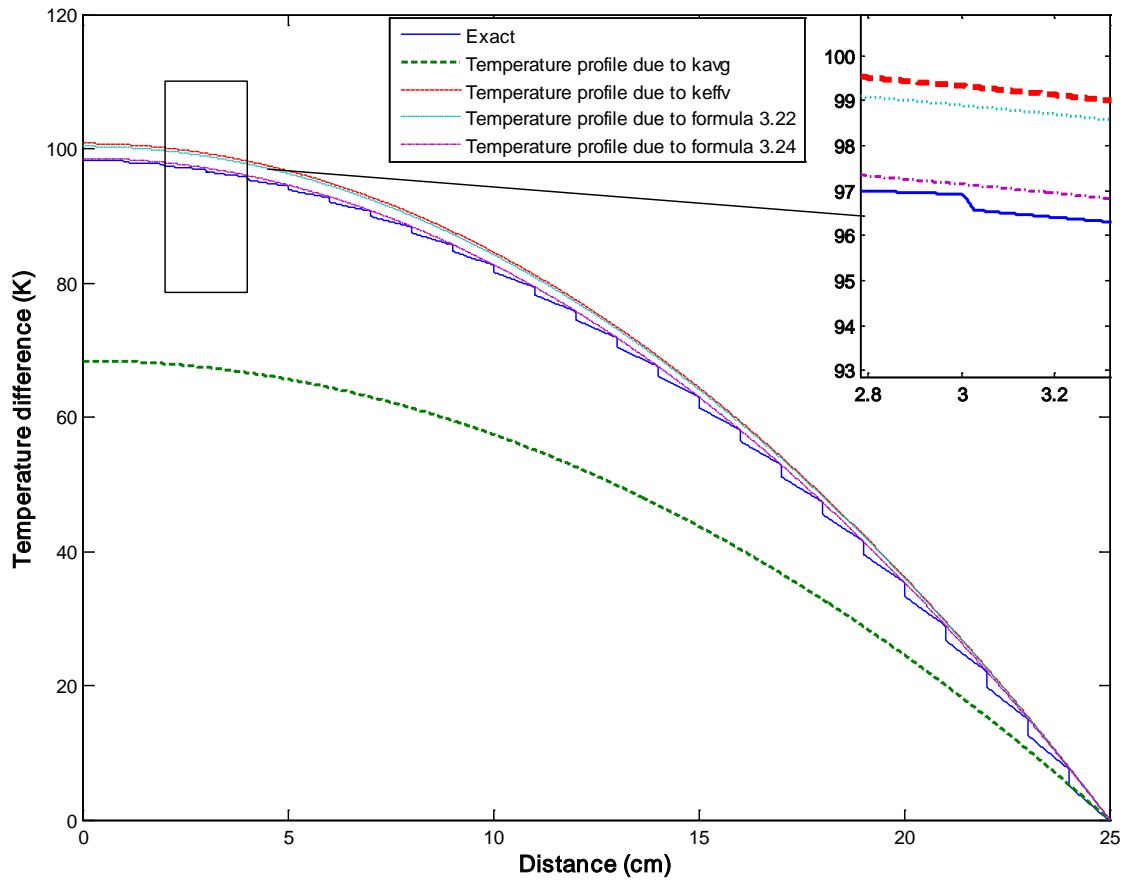


Figure 4.1. Temperature profiles obtained using different estimates for the value of the thermal conductivity.

Figure 4.1 shows the exact temperature profile in the layered sphere and four quadratic profiles. Each quadratic profile corresponds to one of the homogenized thermal conductivities discussed above. The figure shows that the simple volume weighted thermal conductivity gives the largest error. On the other hand, the other three thermal conductivities give a fairly good approximation to the exact temperature profile.

### 4.3 Fuel-Moderator Layered System Representing the PBMR Fuel

For a comprehensive evaluation of our approach, homogenized conductivity values are compared to the values of a homogenized thermal conductivity predicted by the empirical correlation reported by Gao and Shi [8] and discussed in section 2.2.2. Such a comparison provides an assessment of both the structural (layered) approximation as well as the empirical (quadratic) formulation used in our approach.

A challenge in carrying out this comparison is to know the exact composition of the fuel pebble for which the empirical correlation given by Eq. 2.9 was developed. All efforts to find this information from the open literature were unsuccessful. Hence, we are forced to look at different possible material and configurations. Two efforts are to identify the type of graphite used in the development of the empirical correlation, and to find out the graphite to fuel volumetric ratio.

To address the issue of the type of graphite used in the pebble fuel, we looked at several different types of graphite. Correlations for the thermal properties of several of these extracted from different sources are given in Appendix A. In their report “Performance Evaluation of Modern HTR TRISO Fuels”, Gontard and Nabielek [4] suggested that to meet the specification requirements for the High Temperature Reactor, both the 5 mm thickness fuel-free graphite shell and the 50 mm diameter graphite zone in which the fuel particles are dispersed are based upon the matrix A3 graphite. However, there is some doubt about this claim since the thermal conductivity predicted by the correlation reported by Gao and Shi [8] for the composite material is higher than that of A3. In fact, for all temperatures, the thermal conductivity of both types of A3 graphite (A3-3 and A3-27) is lower than the thermal conductivity of the homogenized value predicted by the correlation reported by Gao and Shi [8]. (Since the thermal conductivity of the TRISO fuel is much lower than the thermal conductivity of graphite; the thermal conductivity of the composite material as a homogenized medium—which is expected to be in between the values of the two component thermal conductivities—must be lower than the thermal

conductivity of pure graphite.) Table 4.6 shows the thermal conductivities for different types of graphite at different temperatures. It also shows the thermal conductivities at different temperatures as predicted by Eq. 2.9 (for DOSIS = 0).

Table 4.6. Thermal conductivities of different types of graphite and thermal conductivity calculated using Eq. 2.9 at different temperatures.

Temperature ( $^{\circ}C$ )	Thermal conductivity $W/(m.K)$				
	Matrix Graphite A3-3 (Cured at $1950^{\circ}C$ )	Matrix Graphite A3-3 Cured at $1800^{\circ}C$ )	Matrix Graphite A3-27 (Cured at $1950^{\circ}C$ )	Matrix Graphite A3-27 (Cured at $1800^{\circ}C$ )	As given by the correlation reported by Gao and Shi [8]
100	64.60	50.80	62.20	47.40	73.71
400	45.62	37.65	43.62	36.50	48.97
600	38.22	32.07	36.65	31.30	41.06
800	33.79	28.38	32.68	27.43	36.44
1000	31.57	26.16	30.88	24.64	33.83

Examining the thermal conductivities of two different types of matrix A3 graphite (A3-3 and A3-27) tabulated in Table 4.6 we find that the matrix graphite A3-3 cured at  $1950^{\circ}C$  has the highest thermal conductivities. Though they are still less than the thermal conductivity predicted using Eq. 2.9 for the composite (graphite and TRISO fuel particles) system, nevertheless, matrix graphite A3-3 (cured at  $1950^{\circ}C$ ) appears to have the highest potential to be the graphite used in the fuel for which Eq. 2.9 was developed.

Another difficulty in comparing the homogenized conductivity predicted by Eq. 2.9 to the results from our analysis is in determining the exact abundance of the fuel in the pebble. In their report,

Gontard and Nabielek [4] suggest the number of fuel particles dispersed in the graphite matrix to be over 20,000. We assumed 20,000 particles with dimensions discussed in Section 1.2, and determined the volumetric ratio of the fuel to the moderator (represented by the ratio  $t_f/t_m$  in our equations) to be 0.02041.

As an approximation uranium dioxide ( $UO_2$ ) was used as the fuel material (ignoring other layers of graphite and SiC). Expressions for the thermal conductivity of both uranium dioxide and A3 graphite matrix are given in Appendix A. With the type of graphite and the fuel to graphite volumetric ratio determined, the homogenized thermal conductivity of the PBMR fuel was determined using Eqs. 3.16 and 3.24.

Table 4.7. Comparison of results for homogenized thermal conductivity with those predicted by the correlation reported by Gao and Shi [8].

Temperature (°C)	Thermal conductivity of Graphite A3-3 W/(m.K)	Thermal conductivity of Uranium Dioxide W/(m.K)	Thermal conductivity as given by the correlation reported by Gao and Shi [8]. W/(m.K)	Thermal conductivity given by Eqs. (3.16) and (3.24) W/(m.K)	Relative Error (percent)
400	45.62	5.4584	48.97	40.39	17.52
600	38.22	4.415	41.06	33.68	17.97
800	33.79	3.7074	36.44	29.57	18.85
1000	31.57	3.2014	33.83	27.30	19.30
Average Error (percent)					18.41

Table (4.7) shows the thermal conductivities for four values of temperatures as predicted by the correlation reported by Gao and Shi [8] in the fourth column, and thermal conductivities as calculated by our empirical expression, in the fifth column. The last column has errors between the two values. The average discrepancy is found to be 18.41 percent.

Assumptions made for the type of graphite used and the abundance of fuel in the sphere are two potential sources of discrepancy in the results shown in Table (4.7). Other possible reasons are to be sought in the assumptions and approximations made in the development of the expression to determine the homogenized thermal conductivity. Largest of these in this case of a spherical fuel pebble is the 3-D effect on the effective thermal conductivity. In 1-D serial representation of different materials, the thermal conductivity of the material with smaller  $k$  gets a higher weight than it would get if a 3-D analysis was carried out (in which heat could flow through the higher thermal conductivity material by passing through the lower  $k$  material). At least a two dimensional analysis will need to be carried out to capture this effect on the equivalent thermal conductivity. These and other possible extensions of the current work are discussed in the next chapter.

## CHAPTER 5

### SUMMARY, CONCLUSIONS AND FUTURE WORK

#### 5.1 Summary and Conclusions

The thermal conductivity is an important material property to be considered when studying the thermal behavior of a system. It also has a major effect on the fuel performance. For High Temperature Reactors (HTRs), fuel is composed of BISO and TRISO particles dispersed uniformly in a graphite matrix. This composite nature of the fuel makes it hard to determine the effective thermal conductivity of the pebble fuel as a single homogenized material. Since the simple volume weighted thermal conductivity does not agree with experimentally determined effective thermal conductivity of the system, an empirical approach has been suggested in this thesis to predict the thermal conductivity of such mixed materials.

Binary mixed materials were first approximated by layered systems of two alternating fuel and moderator layers. An empirical approach was then adopted to formulate an expression for the effective thermal conductivity of the layered system with heat generation. The structural approximation (the layered model approximation) was first tested for binary mixed materials with no heat generation by using an expression for the effective thermal conductivity derived using this approximation (Eq. 3.7). Results were then validated by comparing them to the experimental results as found by Deng [6] for the effective thermal conductivity of mixed porous media. Three mixed materials were considered in this comparison, fine sand with white lime, fine sand with coal powder and salt with sawdust. This comparison showed a good agreement between the two sets of results. The deviation from the experimental data increased as the difference between the values of the thermal conductivities of the two materials under study was increased. Hence, the error was maximum for the mixture of salt with sawdust and minimum for the mixture of fine sand with coal powder.

A layered system of alternating fuel and moderator layers was then examined. A volume weighted thermal conductivity was proposed using modified volumetric ratios rather than the actual volumetric ratios of the fuel and the moderator in the assembly. Optimum values for these modified volumetric ratios were calculated by matching exact temperature profiles with the homogenized ones.

The values for the optimal modified volumetric ratios were found to converge when the ratio of the thickness of individual layers to the dimensions of the whole system decreases. A parametric study was then performed on the optimal values for those modified volumetric ratios. This parametric study showed that the heat generation rate and the boundary conditions have minimal effect on the final expression for the effective thermal conductivity. This is an expected result because thermal conductivity is a material property and should only depend on the properties of the material's composition. Two other parameters were found to contribute in the final expression for  $k$ , namely, the abundance and the thermal conductivity of each individual component.

Final empirical expressions were assessed by solving numerically for the temperature profile in a binary layered system of fuel and moderator and comparing it to the homogenized temperature profiles. Results showed a smaller error compared to the case of a simple volume weighted thermal conductivity.

The entire approach was then assessed by applying its results to the pebble fuel in a pebble bed reactor. Thermal conductivities evaluated using the final empirical expression were compared to conductivities evaluated using a correlation reported by Gao and Shi [8] and presented in Section 2.2.2. For this comparison, the composition of the fuel spheres was assumed to be matrix A3-3 graphite with pure particles of uranium dioxide of ~2 percent volumetric abundance. Results of this comparison showed an average relative error of 18.41 percent.

## 5.2 Future work

The effort done in this thesis can be further extended to get a better prediction for the effective thermal conductivity for mixed materials of fissile and non-fissile components. This in turn, can ease and enhance the study of the fuel performance and thermal calculations.

A first extension to this work would be by analyzing higher dimensional systems (2D and 3D systems). This will yield a more realistic prediction for the effective thermal conductivity. It can also allow examining systems of higher level of heterogeneity.

A second possible extension is to consider other parameters that might have a direct effect on the thermal conductivity. Temperature and neutron fluence can be examples of such parameters. In an extended analysis, these will appear explicitly in the final expression, rather than appearing implicitly through their effect on the thermal conductivities of the composing materials.

A third possible extension is to extend the analysis by examining systems with different geometries and different composition, like other kinds of fuel that use dispersed fuel kernels in non fissile medium. This extension, along with the first one, will provide the flexibility to choose materials with more complicated geometries, and a composition of more than two materials.

The last suggested extension is to determine the effective thermal conductivity for transient conditions. This will introduce the effects of the densities and the specific heats of the two constituent components as well as their thermal conductivities. This will provide a better understanding of the material's thermal behavior during transients.

# Appendix A

## Physical and Thermal Properties of Some Materials

### 1- Pyrolytic and Porous Graphite:

Table A.1. Thermo-Physical Properties for Pyrolytic and Porous Graphite [10].

Property	Value*
Thermal Conductivity W/(m.K)	$k = 244.3T^{-0.574}[1 - 0.3662(1 - e^{-1.1028\Gamma}) - 0.03554\Gamma][\frac{\rho}{\rho+2.2(1930-\rho)}]$
Density Pyrolytic (kg/m <sup>3</sup> )	1,900
Density Porous (kg/m <sup>3</sup> )	970
Specific Heat J/(kg.K)	$C_p = (0.54212 - 2.42667 \times 10^{-6} T - 90.2725 T^{-1} - 4.34493 \times 10^4 T^{-2} + 1.59309 \times 10^7 T^{-3} - 1.43688 \times 10^9 T^{-4}) * 4184 * [\frac{\rho}{\rho+2.2(1740-\rho)}]$

\* $\Gamma$ : neutron fluence in  $10^{25} \text{ n/m}^2$ , T is in Kelvin

### 2- Grade H-451 Graphite:

Table A.2. Thermal Conductivity of Grade H-451 graphite [10].

Fluence [ $\times 10^{25} \text{ n/m}^2$ ]	Thermal conductivity* [W/(m.K)]
Un-irradiated	$k = 3.28248 \times 10^{-5} T^2 - 0.124890T + 1.69245 \times 10^2$
0.2	$k = 4.56817 \times 10^{-9} T^3 - 3.42932 \times 10^{-6} T^2 - 3.64930 \times 10^{-2} T + 9.01445 \times 10^1$
0.5	$k = 3.33540 \times 10^{-9} T^3 - 7.83929 \times 10^{-6} T^2 - 6.75616 \times 10^{-3} T + 46.6649$
1	$k = 2.03348 \times 10^{-9} T^3 - 5.51300 \times 10^{-6} T^2 - 1.55010 \times 10^{-3} T + 30.5337$
3-8	$k = 1.20901 \times 10^{-6} T^2 - 7.56914 \times 10^{-3} T + 29.8193$

\* Range of validity [500K – 1800K], T in K

Table A.3. Some Thermo-Physical Properties of Grade H-451 graphite [10].

Property	Value*
Density ( $\text{kg/m}^3$ )	1,740
Specific Heat J/(kg.K)	$C_p = 4184 (0.54212 - 2.42667 \times 10^{-6} T - 90.2725 T^{-1} - 4.34493 \times 10^4 T^{-2} + 1.59309 \times 10^7 T^{-3} - 1.43688 \times 10^9 T^{-4})$
Emissivity	0.85

\* T in Kelvin

### 3- Grade 2020 Graphite:

Table A.4. Thermal Conductivity of Grade 2020 graphite [10].

Fluence [ $\times 10^{22} \text{ n/m}^2$ ]	Thermal conductivity* [W/m/K]
Un-irradiated	$k^* = 1.71039 \times 10^{-7} T^3 - 3.73458 \times 10^{-4} T^2 + 0.218725 T + 26.541$
0.4	$k^{**} = 5.89227 \times 10^{-5} T^2 - 0.128522 T + 111.808$
1	$k^{**} = 7.53255 \times 10^{-6} T^2 - 3.46161 \times 10^{-2} T + 69.8153$
4	$k^{**} = -1.26995 \times 10^{-5} T^2 + 1.08450 \times 10^{-2} T + 43.2150$
10	$k^{**} = -2.87164 \times 10^{-5} T^2 + 4.83551 \times 10^{-2} T + 20.2541$
20	$k^{**} = -4.29785 \times 10^{-5} T^2 + 8.18658 \times 10^{-2} T - 0.713659$

\* Range of validity [295K – 1073K]

\*\* Range of validity [673K – 1073K]

Table A.5. Some Thermo-Physical Properties of Grade 2020 graphite [10].

Property	Value*
Density ( $\text{kg/m}^3$ )	1,780
Specific Heat J/(kg.K)	$C_p = (0.54212 - 2.42667 \times 10^{-6} T - 90.2725 T^{-1} - 4.34493 \times 10^4 T^{-2} + 1.59309 \times 10^7 T^{-3} - 1.43688 \times 10^9 T^{-4}) * 4184 * [\frac{\rho}{\rho + 2.2(1740 - \rho)}]$
Emissivity	0.85

\* T in Kelvin

#### 4- Matrix Graphite [4]:

$$k \text{ W/(cm. } ^\circ\text{C)}^* = k_{100} [1 - \alpha(T - 100) \cdot e^{\delta T}] \cdot [1 - \gamma(1 - e^{-\beta \Gamma}) - \varepsilon \Gamma]$$

$$\gamma = 0.94 - 0.604E - 3T$$

$$\beta = 2.96 - 1.955E - 3T$$

$$\varepsilon = 0.043E - 3T - 0.008 \cdot \left(\frac{T}{1000}\right)^8$$

Table A.6. Constants for matrix graphite.\*\*

Constant	A3-3 1800 °C	A3-3 1950 °C	A3-27 1800 °C	A3-27 1950 °C
$k_{100}$	0.508	0.646	0.474	0.622
$\alpha$	$1.181 \times 10^{-3}$	$1.4079 \times 10^{-3}$	$9.7556 \times 10^{-4}$	$1.4621 \times 10^{-3}$
$\delta$	$-7.8453 \times 10^{-4}$	$-9.0739 \times 10^{-4}$	$-6.036 \times 10^{-4}$	$-9.605 \times 10^{-4}$

\*  $\Gamma = \text{Fluence } [ \times 10^{25} \text{ n/m}^2 ]$

\*\* Temperatures in the first row are curing temperatures

Thermal conductivities of Graphite matrix A3-3 and A3-27 for zero fluence at different temperatures and cured at different temperatures are shown in fig. A.1

#### 5- Silicon carbide (SiC):

Table A.7 Thermo-Physical Properties for SiC [10].

Property	Value
Thermal Conductivity W/(m.K)	$k_{unirr} = \left(2 + \frac{17885}{T}\right) e^{-0.1277\Gamma}$
Density PyC (kg/m <sup>3</sup> )	4,210

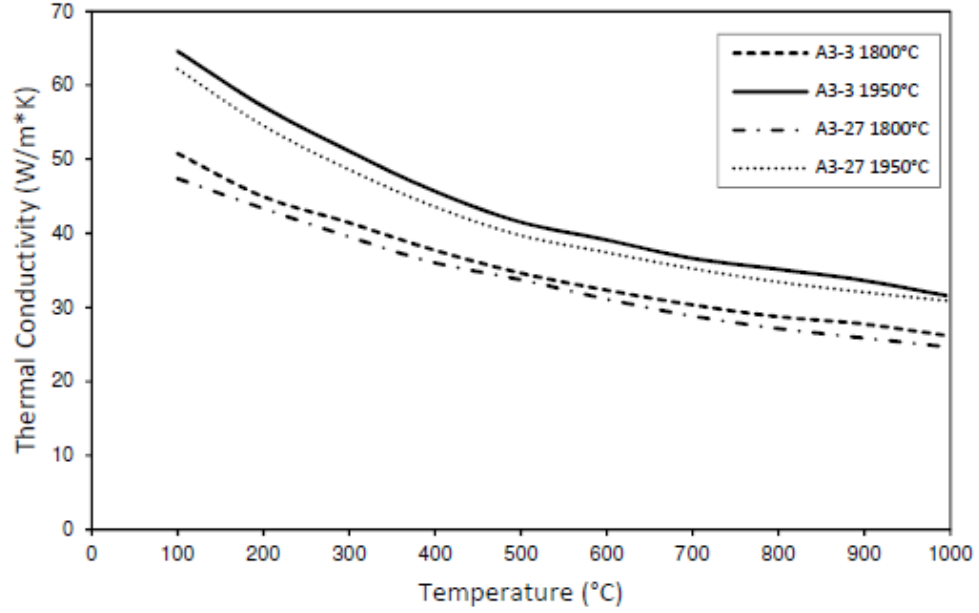


Figure A.1. Thermal conductivities of graphite matrix A3-3 and A3-27 for zero fluence at different temperatures (for different curing temperatures) [4].

## 6- Uranium Dioxide ( $UO_2$ ):

Thermal conductivity for uranium dioxide as developed by Harding and Martin [9] is given by:

$$K_{UO_2} = (0.0375 + 2.165 \times 10^{-4}T)^{-1} + (4.715 \times 10^9 T^{-2} \times e^{-16361/T})$$

where  $K_{UO_2}$  in W/(m.K) and T in Kelvin.

## Appendix B

### Experimental Thermal Conductivities for Mixtures of Porous Materials

Values for the thermal conductivity of the three porous mixtures as reported by Yueying Deng [6] (1990) are shown in Table (B.1), Table (B.2) and Table (B.3) below:

Table B.1. Thermal conductivities of mixtures of fine sand and white lime [6].

Volumetric fraction of fine sand	Thermal conductivity $\lambda$ kcal/(m.h.°C)	Dry bulk density $\rho$ (kg/m <sup>3</sup> )
0	0.194	796
0.091	0.194	791
0.167	0.2	883
0.375	0.196	1016
0.444	0.22	1084
0.5	0.221	1140
0.526	0.224	1166
0.556	0.222	1204
0.588	0.25	1232
0.625	0.262	1277
0.667	0.292	1304
0.714	0.301	1359
0.769	0.313	1412
0.833	0.311	1432
0.909	0.323	1468
1	0.336	1510

Table B.2. Thermal conductivities of mixtures of fine sand and coal powder [6].

Volumetric fraction of fine sand	Thermal conductivity $\lambda$ kcal/(m.h.°C)	Dry bulk density $\rho$ (kg/m <sup>3</sup> )
0	0.199	715
0.091	0.208	764
0.231	0.208	907
0.375	0.223	1033
0.5	0.23	1091
0.526	0.237	1110
0.556	0.243	1137
0.588	0.253	1153
0.625	0.271	1187
0.667	0.277	1217
0.714	0.285	1261
0.769	0.311	1293
0.833	0.321	1346
0.909	0.332	1396
1	0.336	1510

Table B.3. Thermal conductivities of mixtures of salt and sawdust [6].

Volumetric fraction of salt (percent)	Thermal conductivity $\lambda$ kcal/(m.h.°C)	Dry bulk density $\rho$ (kg/m <sup>3</sup> )
0	0.082	106
0.091	0.099	207
0.231	0.096	381
0.333	0.131	503
0.412	0.159	595
0.5	0.177	689
0.526	0.165	718
0.555	0.191	767
0.588	0.217	800
0.625	0.257	829
0.666	0.243	858
0.714	0.263	900
0.769	0.288	946
0.833	0.338	987
0.909	0.381	1048
1	0.394	1119

## Appendix C

### MatLab Code

This code was used to calculate the effective thermal conductivity of a layered spherical assembly for different volumetric ratios of the fuel and the moderator, represented by  $t_f$  and  $t_m$ . Results obtained using this code were analyzed and discussed in Chapter 3.

```
clear;
clc;

layer=input('enter the number of the total assembly layers?')

%-----
%--- Material Properties
%-----
kf=0.01;          %Thermal conductivity of 1st material (fissile material)W/(cm.K)
km=0.21;          %Thermal conductivity of 2nd material (non-fissile material) W/(cm.K)
h=0.5;           %Heat transfer coefficient W/(cm².K)
Tinf=300;         %Temperature at the boundary(K)
q=('enter the heat generation rate?') %Heat generation rate W/cm³
BC= input('choose B.C.: (1 for Drichlet, 2 for Newmann)'); %Boundary condition
dof= input('choose Geometry: (1 for Cylindrical, 2 spherical)');
val=zeros(19,1);
x=zeros(19,1);
value=1;
tf=input('input first thickness of fuel layers'); %Actual thickness for fissile
                                                    material (cm)

while value<20
tm=1-tf;          %Actual thickness for non-fissile material (cm)

dr=0.0005; %spacial step
Nf=fix(tf/dr);
Nm=fix(tm/dr);
NN=Nf+Nm;
siz=(layer/2)*(Nf+Nm);
L=(layer/2)*(tf+tm);
Th=zeros(siz,1);
T=zeros(siz,1);
Tavg2=zeros(siz,1);
Tavg1=zeros(siz,1);
Tnum=zeros(siz,1);
Topt=zeros(siz,1);
Topt2=zeros(siz,1);
```

```

S=zeros(siz,1);
A=sparse(siz,siz);
R=zeros(layer,1);

for p=1:layer      % position at the end of each layer
    if mod(p,2)==0
        R(p)=((p/2)*(tf+tm));
    else
        R(p)=(0.5*((p+1)*tf)+((p-1)*tm));
    end
end

summation=(R(1))^(dof+1);

for p=2:layer

    if mod(p,2)==1
        summation=(summation+((R(p))^(dof+1)-(R(p-1))^(dof+1)));
    end
end
qh=(q*summation)/(L^(dof+1));

%-----
%--- Solving for the exact numerical solution
%-----
Sterm= -(q/kf);
for j=1:(layer/2)      % filling the source vector
    for i=2:Nf-1
        S(i+((j-1)*(Nf+Nm)))=Sterm;
    end
end

for i=2:siz-1      %filling the A matrix
    r=((i-1)*dr);
    Af=((dof/(r*dr))+(1/dr^2));
    Bf=(1/dr^2);
    Cf=-((dof/(r*dr))+(2/dr^2));
    Am=((dof/(r*dr))+(1/dr^2));
    Bm=(1/dr^2);
    Cm=-((dof/(r*dr))+(2/dr^2));
    module=mod(i,NN);
    if module<Nf
        A(i,i)=Cf;
        A(i,i-1)=Bf;
        A(i,i+1)=Af;
    elseif module>Nf
        A(i,i)=Cm;
        A(i,i-1)=Bm;
        A(i,i+1)=Am;
    end
end

A(1,1)=1;      % First B.C.

```

```

A(1,2)=-1;
if BC==1
    A(siz,siz)=1;
else
    A(siz,siz)=(1+(km/(h*dr))); % Last B.C.
    A(siz,siz-1)=-(km/(h*dr));
end

S(siz)=Tinf;

for i=1:(layer-1) % setting the terms those were given a value to zero
again
    plus=(i+mod(i,2))/2;
    minus=(i-mod(i,2))/2;
    N=((plus*Nf)+(minus*Nm));
    A(N,N)=0;
    A(N,N-1)=0;
    A(N,N+1)=0;
    A(N+1,N+1)=0;
    A(N+1,N)=0;
    A(N+1,N+2)=0;
end

for i=1:(layer-1) % Other Internal B.C.s
    plus=(i+mod(i,2))/2;
    minus=(i-mod(i,2))/2;
    N=((plus*Nf)+(minus*Nm));
    A(N,N)=1;
    A(N,N+1)=-1;
    if mod(i,2)==0
        A(N+1,N-1)=-km;
        A(N+1,N)=km;
        A(N+1,N+1)=kf;
        A(N+1,N+2)=-kf;
    else
        A(N+1,N-1)=-kf;
        A(N+1,N)=kf;
        A(N+1,N+1)=km;
        A(N+1,N+2)=-km;
    end
end

Tnum=A\S; % Solving for the exact-k temperature

%-----
%--- Solving for the homogenized numerical solution
%-----
for j=1:siz
    rj=(j-1)*dr;
    Tavgl(j)= ((L^2)-(rj^2));
    if BC==1
        Tavgl(j)=Tinf;
    else

```

```

        Tavg2(j)=Tinf+((qh*L)/((dof+1)*h));
    end
end

At=(sum(Tnum)-sum(Tavg2))/(sum(Tavg1));

for i=1:siz
    Th(i)= (At*Tavg1(i))+Tavg2(i);
end

Af=(1/(kf-km))*((qh/((2*(dof+1))*At))-km);
val(value)=(Af/(1-Af));
x(value)=(tf/(1-tf));
value = value+1;
tf=tf+0.001
end
nn =linspace(0,(layer/2)*(tf+tm),siz);

%Plotting the solution
figure(1)
plot(nn,Tnum,nn,Th)
xlabel 'x (cm)'
ylabel 'Temperature (k)'
title 'Temperature Profile'
legend('Numerical','Exact',2);
figure(2)
plot(x,val)
xlabel 'actual ratio'
ylabel 'optimal ratio'
title 'optimal to Actual fuel to moderator ratios'

```

## Appendix D

### Analytical Solution for Temperature in Four-Layered Assembly (Fig. 3.2)

Temperature profiles in layers 1 through 4 in Fig. 3.2 are governed by the differential equations:

$$\frac{d^2 T_1}{dx^2} + \frac{Q}{k_f} = 0 \quad \dots \dots \dots (D.1)$$

$$\frac{d^2 T_2}{dx^2} = 0 \quad \dots \dots \dots (D.2)$$

$$\frac{d^2 T_3}{dx^2} + \frac{Q}{k_f} = 0 \quad \dots \dots \dots (D.3)$$

$$\frac{d^2 T_4}{dx^2} = 0 \quad \dots \dots \dots (D.4)$$

With the boundary conditions:

$$\left. \frac{dT_1}{dx} \right|_{x=0} = 0 \quad \dots \dots \dots (D.5)$$

$$T_1|_{x=a} = T_2|_{x=a} \quad \dots \dots \dots (D.6)$$

$$k_f \left. \frac{dT_1}{dx} \right|_{x=a} = k_m \left. \frac{dT_2}{dx} \right|_{x=a} \quad \dots \dots \dots (D.7)$$

$$T_2|_{x=2a} = T_3|_{x=2a} \quad \dots \dots \dots (D.8)$$

$$k_m \left. \frac{dT_2}{dx} \right|_{x=2a} = k_f \left. \frac{dT_3}{dx} \right|_{x=2a} \quad \dots \dots \dots (D.9)$$

$$T_3|_{x=3a} = T_4|_{x=3a} \quad \dots \dots \dots (D.10)$$

$$k_f \left. \frac{dT_3}{dx} \right|_{x=3a} = k_m \left. \frac{dT_4}{dx} \right|_{x=3a} \quad \dots \dots \dots (D.11)$$

$$T_4|_{x=4a} = 0 \quad \dots \dots \dots (D.12)$$

The four differential equations above have the following general solutions:

$$T_1 = \left( \frac{-Q}{2k_f} \right) x^2 + G1x + G2 \quad \dots \dots \dots (D.13)$$

$$T_2 = G3x + G4 \quad \dots \dots \dots (D.14)$$

$$T_3 = \left( \frac{-Q}{2k_f} \right) x^2 + G5x + G6 \quad \dots \dots \dots (D.15)$$

$$T_4 = G7x + G8 \quad \dots \dots \dots (D.16)$$

From the first boundary condition we conclude that  $G1=0$ , and from the other seven boundary conditions we get the following set of algebraic equations:

$$aG3 + G4 - G2 + \left( \frac{Qa^2}{2k_f} \right) = 0 \quad \dots \dots \dots (D.17)$$

$$k_m G3 + Qa = 0 \quad \dots \dots \dots (D.18)$$

$$2aG3 + G4 - 2aG5 - G6 + \left( \frac{2Qa^2}{k_f} \right) \quad \dots \dots \dots (D.19)$$

$$k_m G3 - k_f G5 + 2aQ = 0 \quad \dots \dots \dots (D.20)$$

$$3aG7 + G8 - 3aG5 - G6 + \left( \frac{9Qa^2}{2k_f} \right) = 0 \quad \dots \dots (D.21)$$

$$k_m G7 - k_f G5 + 3aQ = 0 \quad \dots \dots \dots (D.22)$$

$$4aG7 + G8 = 0 \quad \dots \dots \dots (D.23)$$

Solving the system of algebraic equations above we get the constants G2-G8 as follows:

$$G2 = a^2 Q \left( \frac{3}{k_m} + \frac{1}{2k_f} \right) \dots \dots \dots (D.24)$$

$$G3 = \frac{-aQ}{k_m} \dots \dots \dots (D.25)$$

$$G4 = \frac{4a^2 Q}{k_m} \dots \dots \dots (D.26)$$

$$G5 = \frac{aQ}{k_f} \dots \dots \dots (D.27)$$

$$G6 = a^2 Q \left( \frac{3}{2k_f} + \frac{2}{k_m} \right) \dots \dots \dots (D.28)$$

$$G7 = \frac{-2aQ}{k_m} \dots \dots \dots (D.29)$$

$$G8 = \frac{8a^2 Q}{k_m} \dots \dots \dots (D.30)$$

## References

- [1] Baehr, H. D., Stephan, K., “Heat and Mass Transfer”, second edition, Springer-Verlag, Berlin Heidelberg, 2006.
- [2] Petti, D., Windes, W., “Fuel and Graphite Needs for VHTR, Presentation at the Advanced Test Reactor National Scientific User Facility Users Week 2009”. Idaho National Laboratory, 2009.
- [3] Kania, M.J., Nickel, H. “Performance Assessment of the (Th,U)O<sub>2</sub> HTI-BISO Coated Particle Under PNP/HHT Irradiation Conditions”. KFA Jülich report Jül-1685, ISSN 0366-0885, November 1980.
- [4] Gontard, R. and Nabielek, H., “Performance Evaluation of Modern HTR TRISO Fuels”, No. HTA-IB-05/90, 49-53, 393-397. 1990.
- [5] Woodside, W. and Messmer, J.H., “Thermal Conductivity of Porous Media Unconsolidated Solids”, Journal of Applied Physics, v. 32 (9), 1688-1699, 1961.
- [6] Deng, Y., Fedler, C. B. and Gregory, J., “Predictions of Thermal Characteristics for Mixed Porous Media”, Journal of Materials in Civil Engineering, v. 4 (2), 185-195. May, 1992.
- [7] Cho, N. Z., Yu, H. and Kim, J. W., “Two-Temperature Homogenized Model for Steady-State and Transient Thermal Analyses of a Pebble with Distributed Fuel Particles”, Annals of Nuclear Energy, v. 36 (4), 448-457. May 2009. (Also see: Cho, N. Z., Yu, H. and Kim, J. W., “Corrigendum to: Two-Temperature Homogenized Model for Steady-State and Transient Thermal Analyses of a Pebble with Distributed Fuel Particles”, [Annals of Nuclear Energy, 36 (2009) 448–457]. Annals of Nuclear Energy, v. 38 (8), 1793. May 2011.)

- [8] Gao, Z. and Shi, L., “Thermal Hydraulic Calculation of the HTR-10 for the Initial and Equilibrium Core”, Nuclear Engineering and Design, v. 218 (1-3), 51-64, October 2002.
- [9] Harding, J.H. and Martin, D.G., “A Recommendation for the Thermal Conductivity of UO<sub>2</sub>”, Journal of Nuclear Materials, v. 166 (3), 223-226, 1989.
- [10] Gougar, H., Ortensi, J. & others, “Prismatic Coupled Neutronics/Thermal Fluids Transient Benchmark of the MHTGR-350 MW Core Design: Benchmark Definition”, 2010, Retrieved April 2, 2011 from: <https://mail-attachment.googleusercontent.com>. 38-45.